**The Cryosphere
Discussions**

Long-term contributions of Baffin and Bylot Island Glaciers to sea level rise: an integrated approach using airborne and satellite laser altimetry, stereoscopic imagery and satellite gravimetry

A. S. Gardner[1], G. Moholdt[2], A. Arendt[3], and B. Wouters[4]

[1]Department of Atmospheric, Oceanic and Space Science, University of Michigan, Ann Arbor, Michigan 48109, USA
[2]Institute of Geophysics and Planetary Physics, Scripps Institution of Oceanography, La Jolla, California 92093, USA
[3]Geophysical Institute, University of Alaska, Fairbanks, AK 99775, USA
[4]The Royal Netherlands Meteorological Institute, 3730 AE De Bilt, The Netherlands

Correspondence to: A. S. Gardner (alexsg@umich.edu)

Title Page	
Abstract	Introduction
Conclusions	References
Tables	Figures
◀◀	▶▶
◀	▶
Back	Close
Full Screen / Esc	
Printer-friendly Version	
Interactive Discussion	

Abstract

Canadian Arctic glaciers have recently contributed large volumes of meltwater to the world's oceans. To place recently observed glacier wastage into a historical perspective and to determine the region's longer-term (∼50 years) contribution to sea level, we esti-
5 mate mass and volume changes for the glaciers of Baffin and Bylot Islands using Digital Elevation Models generated from airborne and satellite stereoscopic imagery and elevation postings from repeat airborne and satellite laser altimetry. In addition, we update existing glacier mass change records from GRACE satellite gravimetry to cover the period from 2003 to 2011. Using an integrated approach we find that the rate of mass
10 loss from the region's glaciers increased from $11.1 \pm 1.8\,\mathrm{Gt\,a^{-1}}$ ($-270 \pm 40\,\mathrm{kg\,m^{-2}\,a^{-1}}$) in 1963–2006 to $23.8 \pm 3.1\,\mathrm{Gt\,a^{-1}}$ ($-580 \pm 80\,\mathrm{kg\,m^2\,a^{-1}}$) in 2003–2011. The doubling of the rate of mass loss is attributed to higher temperatures in summer with little change in annual precipitation. Through both direct and indirect effects, changes in summer temperatures accounted for 68–98 % of the variance in the rate of mass loss to which
15 the Barnes Ice Cap was found to be 1.6 times more sensitive than either the Penny Ice Cap or the regions glaciers as a whole. Between 2003 and 2011 the glaciers of Baffin and Bylot Islands contributed $0.07 \pm 0.01\,\mathrm{mm\,a^{-1}}$ to sea level rise, a rate equivalent to the contribution coming from Patagonian glaciers. Over the 48-year period between 1963 and 2011 the glaciers of Baffin and Bylot Islands contributed 1.7 mm to the world's
20 oceans.

1 Introduction

The glaciers of the Canadian Arctic Archipelago have recently experienced a sharp increase in mass wastage in response to anomalously high summer temperatures (Gardner et al., 2011). Between 2006 and 2009 the glaciers of this region lost ice at a rate
25 of $92 \pm 12\,\mathrm{Gt\,a^{-1}}$, making it the largest contributor to eustatic sea level rise outside of the ice sheets. Of the roughly $147\,000\,\mathrm{km^2}$ of ice in the Canadian Arctic Archipelago,

one third is located on the southern islands of Baffin and Bylot (Fig. 1). Between 2003 and 2009 these glaciers lost ice at an area-averaged rate 1.6 times greater than the glaciers to the north and twice the rate previously estimated by Abdalati et al. (2004) for the period 1995–2000. Apart from the two short periods of 1995–2000 and 2003–2009,

5   little is known about changes in glacier mass for this region.

Here we focus on glaciers of Baffin and Bylot Islands in order to construct a more complete picture of the spatial patterns of glacier change, and to determine the region's long-term (∼50 years) contribution to sea level rise, thereby placing recently observed mass loss rates into a historical context. In previous works (Gardner and Sharp, 2009;

10   Gardner et al., 2011) a surface mass budget model has been used to simulate the long-term glacier mass changes for the northern Canadian Arctic Archipelago. Applying the same model to simulate long-term glacier changes of Baffin and Bylot Islands was not possible due to a paucity of on-glacier climate observations. We instead construct long-term glacier mass change from changes in elevation that are determined

15   from historical aerial photogrammetry, modern satellite stereoscopic imagery and repeat airborne and satellite laser altimetry. The measured elevation changes were then extrapolated to regional volume changes and converted to mass changes. For completeness, we provide an update to Gardner et al.'s (2011) 2003–2009 estimates of glacier mass change derived from repeat satellite gravimetry by including the years

20   2010 and 2011.

Through our data integration efforts we are able to assess the extent to which sparse elevation change measurements, in particular those determined from satellite and airborne laser altimetry, can be used to characterize regional-scale glacier change. In addition, multi-temporal estimates of mass change in combination with long-term me-

25   teorological records allow us to identify the primary climatic drivers of glacier mass change for this region.

A. S. Gardner et al.

Title Page

Abstract | Introduction

Conclusions | References

Tables | Figures

|◄ | ►|

◄ | ►

Back | Close

Full Screen / Esc

Printer-friendly Version

Interactive Discussion

2 Study Region

Baffin Island is located to the north of Quebec and Labrador in the territory of Nunavut, Canada (Fig. 1). It covers an area of 507 000 km^2, making it the largest island in the Canadian Arctic Archipelago and one of the five largest islands in the world. To the northeast lies the heavily glaciated and uninhabited Bylot Island. The glaciers of the two islands cover a total area of 41 000 km^2 (year ~2000: Fig. 1). The mountainous eastern coast of the region is clustered with icefields and small ice caps (23 700 km^2 on Baffin and 4900 km^2 on Bylot) within a ~100 kilometers distance from the ocean (Fig. 1). Extending farther inland on Baffin Island, there are two major ice caps, Barnes and Penny, that cover an area of 5900 km^2 and 6500 km^2, respectively. Baffin Island is of particular glaciological importance as it played a central role in the initiation of the of the Laurentide Ice Sheet some 116 thousand years ago (Clark et al., 1993), the remnants of which still exist today in the two large ice caps (Hooke, 1976; Fisher et al., 1998; Zdanowicz et al., 2002).

Scientific research on the glaciers of this region first began in the early 1950s and has focused primarily on the two major ice caps (Ward, 1954; Orvig, 1954, 1951; Baird, 1952). Only a handful of in situ conventional and geodetic glacier observations exist for the Barnes Ice Cap (1950; Ward, 1954; 1962–1966; Sagar, 1966; 1965–1966; Løken and Sagar, 1967; 1970–1984; Hooke et al., 1987 and 1984–2006; Sneed et al., 2008), the Penny Ice Cap (1953; Ward, 1954; 2008-present; Geological Survey of Canada) and a small valley glacier situated to northeast of the Penny Ice Cap (1969–1976; Weaver, 1975). There are also observations of modern changes in the margin positions of the Barnes Ice Cap (Jacobs et al., 1993, 1997) and some 662 glaciers located on the Cumberland Peninsula, southern Baffin Island (Paul and Svoboda, 2009). For Bylot Island, a comprehensive study of late 1800s, 1958/61 and 2001 valley glacier extents was completed by Dowdeswell et al. (2007). These local studies indicate that the glaciers of Baffin and Bylot Island have been in a state of mass loss and retreat since at least the 1950s.

Title Page

Abstract	Introduction
Conclusions	References
Tables	Figures

⏮   ⏭

◀   ▶

Back   Close

Full Screen / Esc

Printer-friendly Version

Interactive Discussion

The first regional estimate of glacier mass change was done by Abdalati et al. (2004) using repeat airborne laser altimetry collected over the Barnes and Penny Ice Caps in spring-1995 and spring-2000. Assuming that the measured elevation change gradients were representative of all glaciers in the region, they estimated that the glaciers of Baffin Island had lost ice at an average rate of $-10.2\,\mathrm{Gt\,a^{-1}}$ (assuming an ice density of $900\,\mathrm{kg\,m^{-3}}$). More recently, Gardner et al. (2011) used repeat satellite altimetry (ICESat) and gravimetry (GRACE) to show that the rate of ice loss from the entire region (Baffin + Bylot) had more than doubled to $-24\,\mathrm{Gt\,a^{-1}}$ for the period fall-2003 to fall-2009.

3 Data and Methods

3.1 Glacier complex outlines

Outlines of glacier complexes were compiled from 214 individual CanVec maps, a digital cartographic reference product produced by Natural Resources Canada (acquired from: www.GeoGratis.gc.ca). An additional $5500\,\mathrm{km^2}$ of glacier area not covered by Edition 9 of the CanVec data set was taken from an expanded inventory of Paul and Svoboda (2009). All outlines are based on late-summer Landsat imagery acquired between 1999 and 2004 with the exception of 13 CanVec maps that used late-summer SPOT 5 imagery acquired between 2006 and 2010 and 7 CanVec maps that used 1958 or 1982 aerial photographs. We visually checked the glacier outlines against late-summer Landsat imagery. Some manual editing was done to reclassify a small fraction of ice coverage (<1 %) that was missed by the CanCev data set due to incorrect classification over debris cover and supraglacial lakes. The overall quality of the data set was found to be very high.

The new glacier inventory gives a total ice covered area of $36\,100\,\mathrm{km^2}$ for Baffin Island and $4900\,\mathrm{km^2}$ for Bylot Island (Fig. 1). These areas are respectively $2 \pm 2\,\%$ and $4 \pm 3\,\%$ smaller than a range estimates published in the 1950s and 1960s (see Table 2

in Ommanney, 1971). The smaller area of our data set is attributed to both long-term glacier retreat and methodological differences in glacier delineation.

3.2 Elevation Data Sets:

To determine changes in glacier elevations through time we difference a number of elevation products. We use Canadian Digital Elevation Data (CDED) for historical (1952–1983) elevations and for modern elevations we use SPOT 5 HRS Digital Elevation Models (DEMs: 2008–2010), ICESat satellite laser altimetry (2003–2009), and NASA IceBridge Airborne Topographic Mapper laser altimetry (1995–2011). The data sets have varying temporal and spatial coverage and are generated using different methods.

3.2.1 Historic Canadian Digital Elevation Data (CDED)

Canadian Digital Elevation Data (CDED) was provided at a scale of 1:50 k. Horizontal coordinates are in North American Datum 1983 (NAD83) and elevations are orthometric with respect to the Mean Sea Level of the Canadian Vertical Geodetic Datum of 1928 (CVGD28). The data set has a horizontal resolution of 23 m in the north-south direction and 8–17 m in the east-west direction. We used Edition 3.0 of the CDED 1:50 k data set that was created primarily form historical aerial photographs by stereo-compilation using control points from the Canadian Aerial Survey Database. Maps over areas with incomplete air photo coverage or insufficient image contrast (primarily over ice and snow) were created from modern DEMs generated from satellite stereoscopic imagery (SPOT 5) and radar interferometry (ERS). A previous validation of 21 high Arctic CDEDs against ICESat laser altimetry showed the data set to be of high accuracy with a mean offset of +0.34 m above ICESat postings and a standard deviation of 6.22 m (Beaulieu and Clavet, 2009). We preformed a similar assessment of the 340 CDEDs used in this study against plane-filtered ICESat data (see 3.2.3). The CDEDs had a mean offset of +1.1 m above ICESat postings, a standard deviation of 5.1 m, and very

good horizontal control. The exception to this was map sheet 026p03 that covers the south-west margin of the Penny Ice Cap, which we removed from the analysis because of large negative elevation biases relative to ICESat.

At the time of writing, the CDED 1:50k data set was still a work in progress and had incomplete coverage for the Canadian Arctic. Complete CDED coverage was only available at a scale of 1:250k and was created from the digitization of National Topographic System (NTS) maps, however, we found the quality of this data set (-3.2 ± 20.7 m) to be insufficient for elevation change detection.

3.2.2 SPOT 5 Digital Elevation Models (DEMs)

SPOT 5 HRS (High Resolution Stereoscopic) DEMs were provided by the French Space Agency (CNES) through the SPIRIT International Polar Year project (Korona et al., 2009). The DEMs come in two versions with respective reliability masks that were generated with sets of correlation parameters adapted to different types of relief; Version 1 is optimized for gentle terrain and Version 2 is optimized for rugged terrain. The DEMs have a horizontal resolution of 40 m, a ground coverage of 120 km by 600 km, and orthometric elevations referenced to the EGM96 geoid. The DEMs were extracted using a 100 % automatic processing method that included no manual intervention and no interactive check against any kind of ground-based measurements (Korona et al., 2009). The reliability masks provide grid cell correlation scores of the DEM generation and identifies interpolated pixels. Similar DEMs produced for other regions have been found to be highly suitable for elevation change detection over complex glaciated terrain after applying proper bias corrections (Berthier et al., 2007; Berthier et al., 2010).

Two pairs of SPOT DEMs (A & B) were acquired over the Barnes Ice Cap, one pair over the Penny Ice Cap, one pair over the Cumberland Peninsula (directly south of the Penny Ice Cap), one pair over Bylot Island, and one pair over the northeastern tip of Baffin Island. All DEMs were generated from late summer imagery (7 July to 3 October) acquired in either 2008 or 2010 with the exception of the Cumberland Peninsula DEMs that were acquired on 10 March 2010. SPOT elevations were first

referenced to the WGS84 ellipsoid and all interpolated pixels (reliability masks of 0 or >100) were excluded. The accuracy of non-interpolated pixels were then assessed using plane-filtered ICESat elevations (Sect. 3.2.3) acquired within ±90 days of the SPOT acquisition date for ice-covered terrain and all June to October (minimal snow cover)

5 elevations for ice-free terrain. For those DEMs generated from 2010 imagery (Table A1), elevations over ice were taken from the prior year since ICESat was not operational in 2010. From this analysis an optimal reliability masks threshold was individually selected for each of the SPOT DEMs (Fig. A1). Comparisons of valid SPOT elevations against CDED and ICESat altimetry reveal that the SPOT DEMs contain horizontal po-

10 sitioning errors between 7 m and 29 m (Table A2) and elevation biases ranging from −13 m to +5 m (Table A1). Despite the large absolute errors, the relative accuracy of the SPOT DEMs is very good with standard deviations (σ) in the range 2–5 m over ice-free ground and 1–14 m over glacier surfaces with respect to near-coincident ICESat altimetry (Table A1). There is very little difference between DEM versions except for the

15 Barnes_A DEMs, where Version 1 has better coverage and a lower standard deviation over glacier surfaces than Version 2. The SPOT imagery acquired in late August of 2010 (Barnes_B) had much better contrast than the October 2008 imagery (Barnes_A), resulting in fewer interpolated pixels (better coverage) in the Barnes_B DEM. Therefore, the Barnes_A DEM was only used to estimate elevation change for areas not covered

20 by the Barnes_B DEM. There is very little historic (pre-1983) CDED coverage for the north Baffin SPOT DEMs, so we chose to not include the north Baffin DEMs in our glacier elevation change analysis.

3.2.3 Satellite Laser Altimetry (ICESat)

The Geoscience Laser Altimeter System (GLAS) onboard ICESat (Zwally et al., 2002)

25 collected surface elevation profiles over 17 repeated observation campaigns between October 2003 and October 2009. GLAS determines surface elevations from laser pulse footprints that have a diameter of ~70 m at a spacing of ~170 m along each track. We used elevation postings from Release 531 of the GLA06 altimetry product (Zwally et

Long-term contributions of Baffin and Bylot Island Glaciers

A. S. Gardner et al.

Title Page

Abstract	Introduction
Conclusions	References
Tables	Figures

|◄ | ►|

◄ | ►

Back | Close

Full Screen / Esc

Printer-friendly Version

Interactive Discussion

al., 2011b). We converted the data to the WGS84 datum and applied a saturation range correction that is provided with the product. In order to remove potential outlier data from cloud-affected returns, we examined elevation deviations from planes that were fitted 700 m long segments of near repeat-track data (Smith et al., 2009; Moholdt et al., 2010). Elevations that deviated more than 5 m from the calculated plane were excluded from the analysis. In this approach we assume a constant change in elevation with time for each plane when estimated over ice and no change in elevation with time when estimated over ground. Planes were only calculated if they contained a minimum of 4 repeat-track profiles and 10 elevation points. This filtering approach removes about one third of the data, but ensures a data set free of gross errors.

The uncertainty of the filtered ICESat elevations is estimated to be 0.89 m based on the root-mean-square (RMS) difference at 340 northern and southern Canadian Arctic Archipelago crossover points between ascending and descending tracks within individual observation campaigns (<35 days). Similarly, the uncertainty of elevation change rates (dh/dt) determined for planes is 0.36 m a^{-1} based on 296 crossovers. These errors can be due to unresolved surface slopes, temporal variations in rates of elevation change, atmospheric forward scattering, detector saturation, off-nadir pointing and errors in satellite range and positioning (e.g. Siegfried et al., 2011; Fricker et al., 2005; Schutz et al., 2005). Potential systematic errors that might be pertained in all data should be smaller than 0.1 m and 0.01 m a^{-1}, respectively (Zwally et al., 2011a).

3.2.4 Airborne Laser Altimetry (ATM)

Repeat track airborne laser altimetry was conducted over the Barnes and Penny Ice Caps using the NASA IceBridge Airborne Topographic Mapper (ATM) in May and June of 1995, 2000, 2005 and 2011(Barnes Ice Cap only). The ATM system uses a conical scanning laser to measure surface elevations, the footprint and shot spacing of which has changed over time as the ATM hardware has evolved. The system used for the 1995, 2000 and 2005 data has a ∼140 m swath, with each laser shot having a 1–3 m footprint, a ground spacing of 2–5 m, and a nominal accuracy of <0.2 m (Krabill et al.,

2002; Abdalati et al., 2004). The 2011 data were collected with a newer system that has a ~230 m swath, a measurement density of ~1 per 10 m^2, a laser footprint of ~0.5 m and a nominal accuracy of <0.1 m. Because the majority of transects in our study area were flown over relatively featureless ice caps, we used the Icessn product that is a resampled version of the raw laser data (Krabill, 2011). For the Icessn product a block of points are selected at ~0.5 second smoothing interval, which is ~50 m distance along track (actual distance depends on the aircraft speed). The output interval is half the smoothing interval, producing a 50 % overlap between successive platelets. For each smoothing interval there are three platelets produced in the across-track direction, as well as an 80 m platelet located at aircraft nadir. We used all 4 platelets in our elevation change comparisons.

3.3 Elevation change:

Long-term (29–50 years) changes in glacier elevation were determined by differencing historical CDEDs with recent SPOT DEMs and ICESat altimetry. For the Barnes Ice Cap, we also differenced historical CDEDs with ATM altimetry. Short-term (5–16 years) elevation changes were determined through differencing of repeat-track laser altimetry from ATM and ICESat.

3.3.1 SPOT versus CDED

Between 40 and 120 individual 1:50 k CDEDs were mosaiced together to cover each of the 5 pairs of SPOT DEMs. The CDED mosaics were first projected and resampled to the SPOT DEM grid in the UTM map projection of the WGS84 datum. All CDED elevations acquired after 1983 were excluded. The SPOT and mosaiced CDEDs were then co-registered over ice-free surfaces following an iterative process that corrects for the horizontal and vertical offsets using a simple trigonometric relation between aspect, slope and offset (cf. Nuth and Kaab, 2011). To ensure that there is no cumulative

degradation of the elevation data, elevations were resampled from their original sources at each iteration of the co-registration process.

The relative accuracy of the DEMs were investigated by differing the co-registered DEMs from each other over ice-free ground (Table A2). Large elevation differences (dh) were sometimes observed near the modern glacier margins where the ice has retreated over the study period. To make sure that these anomalous values were not included in our examination of ice-free dh, we only included ice-free areas outside of a 1 km buffer surrounding the glaciers. The dh values were then checked and corrected for correlated spatial-, slope-, and elevation-dependent biases over ice-free ground (Fig. A2). The correlated elevation biases were corrected if they improved the standard deviation of dh by 1 % or more. Of these three correlated biases, only spatially correlated biases were detected and corrected for which can result from spatially varying phenomena such as air photo coverage, glacial isostatic adjustment, errors in ground control points and errors in geoid transformations.

After applying bias corrections to the DEMs, we differenced them over glacier surfaces to determine elevation changes (dh) between the CDED and SPOT image acquisition dates. The merged CDED over Bylot Island and the Penny Ice Cap were found to have poor elevation control at higher elevations relative to the SPOT DEMs and ICE-Sat. We removed these errors by applying an iterative standard deviation filter to dh/dt values above 400 m that excludes all values exceeding one standard deviation from the median within 100 m elevation intervals until the standard deviation of each interval is less than 0.3 m a^{-1}. This filter reduced the coverage over ice by about 25 % over Bylot Island, 12 % over the Cumberland Peninsula and 1–6 % elsewhere. Overall the filter has little impact on the area-averaged elevation change (<0.02 m a^{-1}) indicating that errors in the CDED and/or SPOT DEM are likely not biased. The workflow of the SPOT versus CDED co-registration and differencing is provided in Appendix A (Fig. A2).

3.3.2 CDED versus ICESat

The ICESat-CDED differencing follows a similar approach as the SPOT-CDED differencing (Sect. 3.3.1) except that CDED elevations were extracted at ICESat postings by means of bilinear interpolation and we did not apply an iterative standard deviation filter. No significant horizontal misalignment was detected between CDED and ICESat, so the CDED DEMs were only adjusted vertically for a small mean bias (−1.1 m) and spatially correlated biases as determined over ice-free ground (Table A2). A detailed description of the CDED versus ICESat workflow is provided in Appendix A (Fig. A3).

3.3.3 Repeat ATM

Elevation changes for the periods 1995–2000, 2000–2005 and 2005–2011 were calculated from repeat ATM airborne laser altimetry by searching for the closest pairs of platelet centroids from two different campaign years, using a search radius of 100 m (Krabill et al., 2000). We then interpolated the average platelet elevation to the midpoint between the two centroids, based on the reported platelet slopes. Application of this approach to estimate elevation changes of the Greenland Ice Sheet from repeat measurements acquired five years apart were found to have an elevation change error of 0.085 m (Krabill et al., 2002). When averaged over tens of kilometers, this error reduced to 0.07 m. We manually removed a small subset of the 1995–2000 elevation changes that were obvious outliers (elevation changes >200 m).

In 2011 an extensive flight grid was flown over the Barnes Ice Cap that had sufficient sampling of ice-free terrain to allow for vertical co-registration and differencing with historic CDEDs. Following the same methodology as outlined for the ICESat-CDED differencing, we were able to determine 1960–2011 mass changes over the Barnes Ice Cap. We then subtracted the repeat ATM estimates of mass change for the period 1995–2011 to determine the 1960–1995 mass change, hence providing a better time chronology of mass changes for the Barns Ice Cap.

3.3.4　Repeat ICESat

Glacier elevation change rates (*dh/dt*) were calculated from the plane fitting technique as described in Sect. 3.2.3. Due to filtering and data loss in clouds, all planes do not span the entire ICESat repeat-track period from October 2003 to October 2009. We set a minimum time span requirement of 2 years for each *dh/dt*. Additionally, we filtered the start and end campaigns of each plane such that they always span an integer number of years, i.e. our ICESat *dh/dt* estimates are not affected by seasonal biases from accumulation/ablation (Moholdt et al., 2010).

3.4　Mass Change:

3.4.1　From Elevation Changes

Regional rates of volume change (*dV/dt*) were estimated for each elevation change data set by first calculating the mean elevation change rate (*dh/dt*) within each 50 m elevation interval, after applying a 2 sigma filter within each interval to reduce signal noise. Unsampled intervals were linearly interpolated from neighboring values. Intervals above and below the sampled elevation range were set to the median value of the first and last three sampled intervals, respectively. *dV/dt* was then estimated by multiplying the mean *dh/dt* of each elevation interval by the corresponding surface areas within the intervals as determined from the 1:250k CDED. The choice of DEM used for the hypsometrical extrapolation of *dh/dt* has been shown to have little impact on regional volume change estimates (Gardner et al., 2011, supplementary information). The temporal interval of *dV/dt* is determined from the mean date of all valid CDED, SPOT, ICESat and/or ATM elevations. *dV/dt* was then converted into mass change rates (*dM/dt*) by applying a constant glacier density of $900\,\mathrm{kg\,m^{-3}}$.

3.4.2 From GRACE gravimetry

We provide an update to the Gardner et al. (2011) southern Canadian Archipelago (Baffin and Bylot Islands) glacier mass changes derived from repeat gravity observations collected by the Gravity Recovery and Climate Experiment (GRACE) mission.
The GRACE satellites measure the temporal variations of the Earth's geopotential field at a monthly interval, distributed as spherical harmonic coefficients up to degree and order 60, from which the redistribution of surface water masses can be retrieved (Wahr et al., 1998). The spatial resolution of these fields is limited to a few hundred kilometers and the data need to be post-processed and filtered to reduce noise in the observations [see Wouters and Schrama (2007), and Gardner et al. (2011) for a detailed discussion of the processing]. This implies that the GRACE satellites do not make point-observations, but that an observation at a certain location is representative for a larger area. As a result, glacier mass loss cannot be directly obtained by taking a simple area integral over the glacier surfaces. The absence of short wavelength information, in combination with the filtering, will bias the signal within the target area. Additionally, signals from adjacent locations, such as hydrology and glacial isostatic adjustment (GIA), when not properly corrected for, may "leak into" the target area and affect the average (see e.g., Swenson and Wahr, 2002). To counter these problems, we use the iterative method of Wouters et al. (2008): In brief, Baffin and Bylot Islands and the surrounding regions were separated into basins (Fig. S1 of Gardner et al., 2011) to which an initial, random mass anomaly is prescribed (we have verified that final result of the iteration does not depend on the initial values). By applying the same processing steps to these fields as to the real GRACE (CSR LR04) data, pseudo-observations were created and compared to the actual GRACE observations. In an iterative process, the mass anomalies in the basins were adjusted until an optimal agreement in a least-square sense is reached with the GRACE observations.

To isolate the glacier signal, gravity changes associated with GIA were removed using a modified version of the ICE5-G (VM2) model (Peltier, 2004), as described in

Riva et al. (2009). No significant gravity trends due to ice loading and unloading during the Little Ice Age are expected in the region (Jacob et al., 2012). Atmospheric mass variations from European Centre for Medium-Range Weather Forecasts (ECMWF) operational pressure fields are removed by the GRACE science teams during processing of the raw satellite data. Likewise, a baroclinic ocean model in combination with a tide model is used to account for mass variations in the ocean (Bettadpur, 2007). To further reduce ocean effects, we estimated mass anomalies in adjacent ocean basins during the iterative procedure, simultaneously with the glacier and terrestrial water storage variations. Due to the small size of the target area, the signal-to-noise ratio in the time-series is relatively high. As is evident from Fig. 2, interannual changes and trends are very well captured by the GRACE satellites, but the interpretation of month-to-month variations is less straightforward. Therefore, we select the annual value to be the most negative mass value observed at the end of each ablation season (August to September).

3.5 Uncertainty analysis

3.5.1 Mass Changes from Elevation Changes

Sources of uncertainty in our mass change estimates are primarily from uncertainties in: the measurement of dh, dh due to glacial isostatic adjustment, changes in glacier area through time, extrapolation of dh to determine regional dV, mean glacier density and, the changes in the near-surface density profile from changes in compaction rates and internal accumulation. To characterize the measurement uncertainties for long-term differencing that are co-registered over ice-free terrain we examined semivariograms of the elevation difference over non-ice surfaces. After adjusting for identifiable biases there were still large-scale correlations evident in the SPOT-CDED semivariograms, and a more clearly defined correlation length of 50 km in the ICESat-CDED semivariogram, (cf. Rolstad et al., 2009). 50 km is the approximate diagonal length of the largest CDED map used in the study, indicating that dh errors are likely

Long-term contributions of Baffin and Bylot Island Glaciers

A. S. Gardner et al.

correlated by individual CDED map coverage. Therefore, we applied standard error propagation at a correlation length of 50 km to the standard deviation between elevation products over ice-free terrain to estimate the 1σ measurement uncertainty for the ICESat-CDED, SPOT-CDED, and ATM-CDED differencing. For ATM-ATM differencing we assigned a correlated repeat measurement uncertainty of 0.07 m as estimated by Krabill et al. (2002) and for the ICESat-ICESat differencing we assigned an uncertainty of $0.35\,\text{m a}^{-1}$ with an along-track correlation length of 5 km (Moholdt et al., 2010). To account for small biases resulting from glacial isostatic adjustment we added a correlated uncertainty of $3\,\text{mm a}^{-1}$ to all repeat altimetry elevation change estimates (Gardner et al., 2011). This was not necessary for the ICESat-CDED, SPOT-CDED, or ATM-CDED differencing, as elevation products were co-registered over ice-free terrain.

To account for changes in glacier area through time we assigned a conservative 1σ uncertainty of ± 5 % to all dV/dt estimates. The ICESat and ATM differencing have additional uncertainties in dV/dt due to the extrapolation of dh/dt elevation profiles across each region. For the ICESat-CDED and ATM-ATM differencing this was characterized by using subsets of the 2004–2009 ICESat elevation change rates (dh/dt) as analogs for the spatial sampling of dh/dt for the ICESat-CDED and ATM data sets. The dh/dt subsets were selected from a 5 km buffer zone around the ICESat-CDED and ATM postings, respectively. The percentage difference in dV/dt between using all 2004–2009 ICESat data and a subset was then taken as the 1σ uncertainty for the extrapolation from dh/dt to dV/dt. Using this approach we determined uncertainties of 2 % and 16 % for the extrapolation of ATM dh/dt profiles over the Barnes and Penny Ice Caps, respectively. Using ATM dh/dt profiles over the Penny Ice Cap to determine the volume change of the remaining glaciers on Baffin and Bylot Islands introduced an uncertainty of 31 %, which is lower than if data from the Barnes Ice Cap is used. In all cases, extrapolation of the ATM data resulted in an apparent overestimation of mass loss, which indicates that the two ice caps are ablating more rapidly than the coastal icefields. CDED is not complete over the accumulation area of the Penney Ice Cap (Fig. 1), so extrapolation of ICESat-CDED results over the entire ice cap introduced an

uncertainty of 12 %. Similarly, extrapolation of ICESat-CDED results outside of Bylot Island and the two ice caps introduced volume change uncertainties of 3 % and 6 % for the remaining glacier ice to the South and North of 68.6 N, respectively. Volume change uncertainties from the extrapolation of SPOT-CDED results over Bylot Island, the Penny Ice Cap, and the southern glaciers, extrapolation of ICESat-CDED results over Bylot Island and the Barnes Ice Cap and, the extrapolation of ICESat-ICESat results over all regions could not be estimated in the same way as done for the ICESat-CDED and ATM-ATM results. To these estimates we assigned a 1σ extrapolation uncertainty of 5 %.

To convert from *dV/dt* to *dM/dt* we applied a constant glacier density of $900\,\mathrm{kg\,m^{-3}}$ to which we assigned a 1σ uncertainty of $\pm 25\,\mathrm{kg\,m^{-3}}$. This approach assumes a constant rate of compaction and internal accumulation over the past 50 years (i.e. Sorge's law applies; Bader, 1954). This is likely not a valid assumption as rapid changes in glacier mass have recently been observed (Gardner et al., 2011; Fisher et al., 2012). Zdanow-icz et al. (2012) found that there was almost no change in the near-surface (upper 20 m) vertical density-profile between ice cores from 1979 and 1995 collected at elevations of 1975 m and 1860 m on the Penny Ice Cap (Holdsworth, 1984; Fisher et al., 1998). How-ever, comparison with a 2010 core collected at the same location shows that the depth-averaged 20 m density has increased by about $34\,\mathrm{kg\,m^{-3}}$ ($2.2\,\mathrm{kg\,m^{-3}\,a^{-1}}$) since 1995 and is nearly identical to the mean density of a 1953 shallow ice core collected 30 km to the south-southeast at an elevation of 1930 m (Ward, 1954). This suggests that the assumption of a constant density profile is likely appropriate for the multi-decadal ele-vation differences but may introduce errors in shorter-term studies. For example, if the average density of the top 20 m of all glacier areas above the equilibrium line altitude ($\sim$1400 m) increased at a rate of $2.2\,\mathrm{kg\,m^{-3}\,a^{-1}}$, the application of Sorge's law would result in a $0.23\,\mathrm{Gt\,a^{-1}}$ overestimate of glacier mass loss from the region. Unfortunately, the regional changes in firn density are not well enough constrained to justify modify-ing our mass change estimates. We instead assigned a 1σ uncertainty of $2\,\mathrm{kg\,m^{3}\,a^{-1}}$ to areas above 1400 m to account for changes in the 20 m density profile for studies

Long-term contributions of Baffin and Bylot Island Glaciers

A. S. Gardner et al.

Title Page

Abstract	Introduction
Conclusions	References
Tables	Figures

◄◄ ►►

◄ ►

Back Close

Full Screen / Esc

Printer-friendly Version

Interactive Discussion

spanning less than 20 years (repeat ATM and ICESat) and $1\,\mathrm{kg\,m^3\,a^{-1}}$ for studies spanning 20 years or more (comparisons with CDED). Note that this uncertainty comes in addition to the uncertainty in mean density ($\pm 25\,\mathrm{kg\,m^{-3}}$).

To determine the total uncertainty we assumed that all individual sources are correlated in space but uncorrelated with each other; i.e. the total uncertainty for each region was taken as the root sum of squares (RSS) of individual uncertainties and the uncertainty in mass change for all ice area was taken as the RSS of the sum of the individual uncertainties. All uncertainties associated with the derivation of mass changes from the various elevation change products are provided in Table 1 as mass equivalent rates ($\mathrm{Gt\,a^{-1}}$).

3.5.2 Mass Changes from GRACE Gravimetry

The GRACE trends in the Arctic region are dominated by the mass change signal of the Greenland Ice Sheet that may affect the retrieval of the mass variations over Baffin and Bylot Islands. Simulations with pseudo-observations based on a combination of models, representative for mass variations in the cryosphere, terrestrial water storage and ocean, have shown that the trends in glacier mass for Baffin and Bylot Islands can be retrieved to within $\pm 3\,\mathrm{Gt\,a^{-1}}$ (Gardner et al., 2011), indicating that our Baffin and Bylot Islands estimates are not significantly affected by the mass loss of the Greenland Ice Sheet.

The geopotential anomalies observed by the GRACE satellites are the sum of mass variations in various components of the Earth system that need to be removed before the glacier mass anomalies can be estimated. Uncertainties in these corrections are included in the overall error bars. We assessed the uncertainty of the atmospheric correction by comparing ECMWF and National Centers for Environmental Prediction Reanalysis (NCEP R1). The trend in atmospheric loading over Baffin and Bylot Islands shows no significant differences between these two products ($0.1 \pm 0.1\,\mathrm{Gt\,a^{-1}}$). Uncertainty in the GIA correction that results from incomplete knowledge of the Earth's

structure and ice loading history is estimated to be 2.5 Gt a^{-1} (1σ) for Baffin and Bylot Islands. This uncertainty was determined by considering a range of realistic viscosity profiles of 0.3×10^{21} to 1×10^{21} Pa s and 0.3×10^{21} to 1×10^{22} Pa s for the upper and lower mantle, respectively, and alternative loading histories (The ICE-3G (Tushingham and Peltier, 1991) and ANU; Lambeck et al., 2004; models). Note that Gardner et al. (2011) erroneously reported a range for the lower mantle viscosity of 0.3×10^{21} to 3.6×10^{21}, this should have been the same as reported here.

Due to the coarse spatial resolution of the GRACE data, the basins used in the iterative basin method do not exactly follow the glacier boundaries and partly cover non-glaciated areas. This means that our results do not only track the glaciers' mass budget, but also changes in terrestrial water storage, since GRACE cannot distinguish between the two. The Global Land Data Assimilation System (GLDAS: Rodell et al., 2004) in its NOAH $0.25° \times 0.25°$ configuration gives a very small trend in terrestrial water storage ($<0.9 \pm 1.2$ Gt a^{-1}) when considering the end-of-melt-season dates that were used to estimate annual mass changes form GRACE (Aug–Sep; see Fig. 2 and Sect. 3.4.2). The trend in terrestrial water storage is small and insignificant so we simply added this to our estimate of uncertainty. In addition to the uncertainties from the GIA and terrestrial water storage, our monthly GRACE solution (Fig. 2) includes measurement error based on sub-set and inter-month comparisons as provided by the GRACE science team. The monthly values differ slightly from those reported in Gardner et al. (2011). This is a result of post-processing of the GRACE data, which relies on EOF analysis and therefore evolves with the period of observation. Differences are well within the error bars of the monthly GRACE solutions.

3.6 Climate

Measurements of surface mass budget and meteorological conditions over glacier surfaces in Baffin and Bylot Islands are both temporally and spatially sparse and do not allow for the calibration/validation of a regional surface mass budget model as employed

by Gardner et al. (2011) for the glaciers in the northern Canadian Arctic Archipelago. That said, there is sufficient weather station data to assess overall regional climate trends. To help interpret glacier mass changes in terms of regional climate forcing, we examined anomalies in mean summer (JJA) homogenized 2 m air temperatures for 4

5 Environment Canada weather stations located at Pond Inlet, Clyde River, Dewar Lakes and Iqualuit (Vincent et al., 2002). We also examined anomalies in adjusted total annual precipitation for the 5 weather stations at Pond Inlet, Nanasivic, Dewar Lakes, Fox Five and Iqualuit (Mekis and Vincent, 2011). Temperature and precipitation records discontinuously span the period 1930 to 2010 and 1932 to 2009, respectively. All stations

10 except Dewar Lakes are located near the ocean and are therefore biased towards lowaltitude coastal conditions (Fig. 1). For this reason, we also examine summer (J,J,A) glacier area-averaged NCEP R1 "free-air" temperature anomalies at 700 mb geopotential height (Kalnay et al., 1996).

4   Results and discussion

15 Long-term elevation changes determined from the comparison of historic CDEDs with ICESat laser altimetry and SPOT DEMs are shown in Figs. 1, 3, 4 and 5, and corresponding mass change estimates are provided in Table 1. The coverage of the Barnes Ice Cap and Bylot Island glaciers is very good for both data sets but coverage elsewhere is limited by CDED and ICESat availability. Merging results form SPOT Barnes_B

20 V2 and Barnes_A V1 DEMs, we estimated that the Barnes Ice Cap lost mass at a rate of $-2.9 \pm 0.3\,\mathrm{Gt\,a^{-1}}$ between 1960 and 2010. This compares well with a rate of $-2.5 \pm 0.3\,\mathrm{Gt\,a^{-1}}$ as estimated from ICESat for the period 1960 and 2006. Most of the difference between the two data sets is likely due to differences in the sampling interval with higher than average losses in the years 2007 through 2010. Despite the ice cap's

25 simple geometry, the map of *dh/dt* reveals a relatively complex pattern of elevation change (Fig. 3). Thinning rates exceed $1.5\,\mathrm{m\,a^{-1}}$ along the northwestern and southwestern margins and at more localized locations along the northeastern margin where

Full Screen / Esc

the ice cap abuts proglacial lakes (i.g. Conn and Bieler Lakes). These proglacial lakes have been shown to locally enhance the ice flow of the Barnes Ice Cap (Andrews et al., 2002). Elevation changes are smallest at higher elevations and for one of the southwest lobes that has likely experienced "local creep slump" (i.e., enhanced ice creep and basal sliding, see Holdsworth, 1977, 1973; Andrews et al., 2002), a phenomena that was also observed by Abdalati et al. (2004) in repeat airborne laser altimetry.

The map of *dh/dt* for the glaciers of Bylot Island generated from the SPOT Bylot V2 DEM and CDED shows a strong pattern of low elevation ablation (Fig. 4). Most outlet glaciers have experienced an average elevation loss of around 1–$2\,\mathrm{m\,a^{-1}}$ at their termini. There are, however, four outlet glaciers (B7, C93, D78, and D20) that experienced little terminus elevation change, suggesting that mass input from glacier flow and accumulation has matched surface ablation over this period. This suggests that these glaciers may have experienced part or all of a surge cycle over the sample interval. This inference is in agreement with Dowdeswell et al. (2007) who found that most of the major outlet glaciers on Bylot Island are surge-type, meaning that at regular intervals they rapidly transport mass from a high elevation reservoir area to a low elevation receiving area. Dowdeswell et al. (2007) also noted that glacier D78, the longest glacier on Bylot Island, had an over-steepened frontal margin and appears to have advanced and overrun it's Neoglacial terminal moraines. This advance is clearly identified in Fig. 4 as an elevation gain at the terminus of D78.

Overall there is a less coherent spatial pattern of glacier elevation change over Bylot Island than observed over the Barnes Ice Cap. This can be attributed to two factors. First, the CDEDs covering glacier ice in this region have a mean date of 1979 and the SPOT DEM was generated from 2008 imagery. This means that the *dh/dt* estimates for Bylot Island cover a period that is 21 years shorter than those derived for the Barnes Ice Cap. Second, glacier elevation change rates are smaller over Bylot Island than over the ice cap. These factors lead to a higher signal-to-noise ratio in the Bylot Island *dh/dt* estimates. From SPOT-CDED differencing we estimated that the glaciers of Bylot Island

lost ice at a rate of $-1.4 \pm 0.4\,\mathrm{Gt\,a^{-1}}$ over the 29 year period. This compares with an estimate of $-1.3 \pm 0.4\,\mathrm{Gt\,a^{-1}}$ as determined from ICESat for the period 1980 to 2006.

Outside of Bylot Island and the Barns Ice Cap the historic CDED coverage is significantly reduced but still sufficient to determine regionally representative *dh/dt* elevation profiles and therefore mass changes for the remaining ice. From SPOT-CDED (Fig. 5) and ICESat–CDED (Fig. 1) differencing we determine mass loss rates of $-1.2 \pm 0.6\,\mathrm{Gt\,a^{-1}}$ (1958–2010) and $-1.6 \pm 0.4\,\mathrm{Gt\,a^{-1}}$ (1958–2006) for the Penny Ice Cap, and $-1.8 \pm 0.3\,\mathrm{Gt\,a^{-1}}$ (1958–2010) and $-1.5 \pm 0.2\,\mathrm{Gt\,a^{-1}}$ (1958–2006) for the $7600\,\mathrm{km^2}$ of glaciers south of 68.6 N excluding the Penney Ice Cap, respectively. From the ICESat–CDED differencing we determine that the $16\,100\,\mathrm{km^2}$ of glaciers north of 68.6 N excluding Bylot Island and the Barnes Ice Cap lost ice at a rate of $-4.1 \pm 0.5\,\mathrm{Gt\,a^{-1}}$ (1963–2006). In total, the glaciers of Baffin and Bylot Islands collectively lost ice at a rate of $-11.1\,\mathrm{Gt\,a^{-1}} \pm 1.8\,\mathrm{Gt\,a^{-1}}$ between 1963 and 2006.

The repeat ATM differencing, starting from 1995, shows higher rates of mass loss for the Barnes and Penny Ice Caps than the long-term average. Between spring of 1995 and 2000 the Barnes Ice Cap lost ice at a rate of $-3.3 \pm 0.2\,\mathrm{Gt\,a^{-1}}$, increasing to $-4.1 \pm 0.3\,\mathrm{Gt\,a^{-1}}$ for the period 2000 to 2005 (Fig. 6), and to $-6.2 \pm 0.4\,\mathrm{Gt\,a^{-1}}$ for the period 2005 to 2011. Similar analysis for the Penny Ice Cap gives mass loss rates of $-1.3 \pm 0.4\,\mathrm{Gt\,a^{-1}}$ for the period 1995 to 2000, increasing to $-2.9 \pm 0.6\,\mathrm{Gt\,a^{-1}}$ for the period 2000 to 2005 (Fig. 7). Unfortunately there were no ATM flights over the Penny Ice Cap in 2011 due to logistical constraints. Extrapolating elevation changes measured over the Penny Ice Cap to the reaming glacier cover gives a total mass loss for the region of $-14.9 \pm 3.6\,\mathrm{Gt\,a^{-1}}$ and $-25.3 \pm 6.4\,\mathrm{Gt\,a^{-1}}$ for the periods 1995–2000 and 2000–2005, respectively. The high uncertainties for the ATM estimates reflect the large area of extrapolation. Comparative extrapolations done with subsets of the 2004–2009 ICESat elevation changes indicate that the ATM estimates are likely negatively biased (see Sect. 3.5.1). That said, we cannot be absolutely certain that the ATM estimates are negatively biased as the ICESat and ATM data sets do not cover the same time period. Abdatali et al. (2004) used the same ATM data to estimate a mass loss

of $-10.2\,\mathrm{Gt\,a^{-1}}$ for the Baffin Island glaciers between 1995–2000. This is 24 % less negative than our corresponding estimate of $-13.4\,\mathrm{Gt\,a^{-1}}$. We largely attribute these differences to our use of an improved glacier mask (1600 km^2 more ice) that likely includes more low-lying glacier ice, the characterization of glacier hypsometry using a much higher resolution DEM, and the calculation of *dh/dt* using the Icessn product that is a resampled version of the raw laser data used by Abdatali et al. (2004).

The recent increase in glacier mass loss is confirmed by near repeat-track ICESat laser altimetry. Our results [updated from Gardner et al. (2011) using new glacier hypsometry] indicate a glacier mass loss of $-25.1 \pm 2.1\,\mathrm{Gt\,a^{-1}}$ for Baffin and Bylot Islands between 2003 and 2009, which is not significantly different from the 2000–2005 ATM estimate. The updated GRACE results for Baffin and Bylot Islands also confirm the increased rates of mass loss (Fig. 2). Between 2003 and 2011 GRACE gives an average mass loss of $-23.8 \pm 3.1\,\mathrm{Gt\,a^{-1}}$. A recent GRACE study (Jacob et al., 2012) find higher rate of loss than we find here (-33 ± 2.5), which may be attributable to the difference in time periods used, the method to estimate mass changes (end-of-melts-season vs. trend of full time series), differences in the terrestrial water storage and GIA correction, etc.. Again, our GRACE values are not significantly different from the 2003–2009 ICE-Sat or 2000–2005 ATM estimates. These results show that the recent rates of glacier wastage, that are more than twice as negative as the long-term average, have been sustained for over a decade.

The interannual variability of snowfall amounts (accumulation) over the glaciers of Baffin and Bylot Islands is small relative to the interannual variability of ablation, and therefore changes in glacier mass budget are well correlated with changes in summer temperature but not as well with changes in precipitation (Hooke et al., 1987; Weaver, 1975). Our analysis of four Environment Canada weather stations shows nearly identical long-term trends in mean summer temperatures of $+0.35 \pm 0.02\,^\circ\mathrm{C}$ per decade (Fig. 8a). Measuring precipitation amounts in the Arctic is notoriously difficult due to gauge undercatch of solid precipitation and difficulties in correcting gauge biases (Mekis and Hogg, 1999). The sparse measurements that are available

Long-term contributions of Baffin and Bylot Island Glaciers

A. S. Gardner et al.

Back | Close

Full Screen / Esc

Printer-friendly Version

Interactive Discussion

Long-term contributions of Baffin and Bylot Island Glaciers

A. S. Gardner et al.

indicate that there has been little change in annual precipitation over the period of study (Fig. 8b). This suggests that the increasingly negative mass budgets in the region have largely been driven by a long-term increase in summer temperature. To support this conclusion we investigated the relationship between mass loss rates and summer glacier area-averaged NCEP R1 700 mb temperature anomalies averaged for each mass change interval (Fig. 9). For the Barnes Ice Cap there is a nearly perfect linear ($r = -0.99$) relationship between the rate of mass change and summer temperatures of $-390\,\mathrm{kg\,m^{-2}\,a^{-1}}$ per $1\,^\circ$C. Mass change rates for the Penny Ice Cap and the region as a whole appear to be less sensitive to changes in summer temperatures (-230 to $-240\,\mathrm{kg\,m^{-2}\,a^{-1}}$ per $1\,^\circ$C, $r = -0.83 - 0.84$). The link between higher summer temperatures and increased glacier ablation is more complex than may first appear. Higher temperatures lead to more downward longwave radiation and increased sensible heat flux, but these direct links can only account for some of the glacier's sensitivity to temperature. Examining NCEP R1 glacier area-averaged summer means we find that for every $1\,^\circ$C increase in 700 mb temperature there is a corresponding $4.7\,\mathrm{W\,m^{-2}}$ increase in the downward longwave radiative flux at the surface. Over a three-month period this is enough energy to melt an additional $110\,\mathrm{kg\,m^{-2}}$ of ice at $0\,^\circ$C. Therefore, increased downward longwave radiation directly account for less than 30 % to 50 % of the observed temperature sensitivity. The remaining sensitivity is due to increased sensible heat flux and indirect effects. One of the largest indirect effects is the temperature-albedo feedback that results in higher absorption of downward shortwave radiative flux. Higher temperatures result in enhanced snow grain growth and larger effective grain sizes that reduce the albedo of snow. This increases shortwave absorption, snow temperature and melt, which in-turn lead to further grain growth (Flanner and Zender, 2006; Gardner and Sharp, 2010). Higher temperatures also result in earlier and more extensive removal of snow. This increases absorption of shortwave radiation by exposing darker glacier ice and firn.

5 Conclusions

Between 1963 and 2006 the glaciers of Baffin and Bylot Islands lost ice at rate of $-11.1 \pm 1.8 \, \mathrm{Gt \, a^{-1}}$ ($-270 \pm 40 \, \mathrm{kg \, m^{-2} \, a^{-1}}$) increasing to $23.8 \pm 3.1 \, \mathrm{Gt \, a^{-1}}$ ($-580 \pm 80 \, \mathrm{kg \, m^2 \, a^{-1}}$) for the period 2003 to 2011. The doubling of the rate of mass loss is attributed to higher temperatures in summer with little change in annual precipitation. The glaciers of Baffin and Bylot Islands are now losing ice at an equivalent rate to the icefields and glaciers of Patagonia (Ivins et al., 2011), both of which are contributing $0.07 \, \mathrm{mm \, a^{-1}}$ to sea level rise. In total, between 1963 and 2011, the glaciers of Baffin and Bylot Islands contributed 1.7 mm to the world's oceans. Summer temperatures accounted for 68–98 % of the variance in the rate of mass change to which the Barnes Ice Cap was found to be 1.6 times more sensitive to than either the Penny Ice Cap or the region as a whole.

Results for the Barnes Ice Cap clearly indicate accelerated rates of mass loss in recent years, 98 % of which can be attributed changes in summer temperature. Results for the Penny Ice Cap, where data coverage is poor, show increased losses but not necessarily acceleration. The good spatial coverage of the SPOT-CDED differencing reveals complex patterns of elevation change for the Barnes Ice Cap and Bylot Island glaciers. Between 2005 and 2011 the Banes Ice Cap lost ice at an area averaged rate of $-1060 \pm 60 \, \mathrm{kg \, m^{-2} \, a^{-1}}$ with enhanced elevation lowering in places where the ice cap abuts proglacial lakes. There are also signs of continued "local creep slump" of the ice cap's southwest lobe. For Bylot Island, the SPOT-CDED differencing reveals a complex pattern of valley-glacier elevation change. Under similar climatic forcing, neighboring valley glaciers show markedly different responses over the past 29 years with one of the glaciers experiencing terminus advance (D78) while the neighboring glaciers retreat. These results highlight that caution should be taken when interpreting climate signals from neoglacial moraines and glacier length records, changes in which are not necessarily a response to changes in recent climate.

Long-term contributions of Baffin and Bylot Island Glaciers

A. S. Gardner et al.

Full Screen / Esc

Printer-friendly Version

Interactive Discussion

In agreement with recent Alaska and Svalbard studies (Nuth et al., 2010; Arendt et al., 2006), our work demonstrate that, with appropriate corrections, regional mass losses can be adequately determined from discontinuous measurements of elevation change. This suggests that the methods used here can potentially be applied to other

5   glaciated areas with poor coverage of elevation data (i.e. use of ICESat and CryoSat at lower latitudes). That said, we find large uncertainties in the extrapolation of ATM elevation change profiles when estimating regional glacier volume changes. This should provide motivation to modify future NASA IceBridge ATM flight lines to have more regionally representative sampling. We also found that after correcting for mean biases

10 in elevation between datasets, the second most important correction was for spatially correlated biases that can result from air photo coverage, spatially varying rates of GIA, control point errors, and geoid transformation errors. Not correcting for this additional source of error can result in large errors in elevation/mass change estimates.

Appendix A

15 **Validation of SPOT DEMs using ICESat data is provided in Table A1 and a detailed comparison of CDED with ICESat and SPOT elevations is provided in Table A2. Elevation differencing workflows are provided in Fig. A1 thought A3.**

References

Abdalati, W., Krabill, W., Frederick, E., Manizade, S., Martin, C., Sonntag, J., Swift, R., Thomas, R., Yungel, J., and Koerner, R.: Elevation changes of ice caps in the Canadian Arctic Archipelago, J. Geophys. Res., 109, F04007, doi:10.1029/2003JF000045, 2004.

Andrews, J. T., Holdsworth, G., and Jacobs, J. D.: Glaciers of the Arctic Islands. Glaciers of Baffin Island, USGS USGS Professional Paper 1386-J-1, J162-J198, 2002.

Arendt, A., Echelmeyer, K., Harrison, W., Lingle, C., Zirnheld, S., Valentine, V., Ritchie, B., and Druckenmiller, M.: Updated estimates of glacier volume changes in the western Chugach Mountains, Alaska, and a comparison of regional extrapolation methods, J. Geophys. Res.-Earth, 111, F000436, doi:10.1029/2005jf000436, 2006.

Bader, H.: Sorge's law of densification of snow on high polar glaciers, J. Glaciol., 2, 319–323, 1954.

Baird, P. D.: The Baffin Island Expedition, 1950, Geogr. J., 118, 267–277, 1952.

Beaulieu, A. and Clavet, D.: Accuracy Assessment of Canadian Digital Elevation Data using ICESat, Photogram. Eng. Remote Sens., 75, 81–86, 2009.

Berthier, E., Arnaud, Y., Kumar, R., Ahmad, S., Wagnon, P., and Chevallier, P.: Remote sensing estimates of glacier mass balances in the Himachal Pradesh (Western Himalaya, India), Remote Sens. Environ., 108, 327–338, 2007.

Berthier, E., Schiefer, E., Clarke, G. K. C., Menounos, B., and Remy, F.: Contribution of Alaskan glaciers to sea-level rise derived from satellite imagery, Nat. Geosci., 3, 92–95, doi:10.1038/ngeo737, 2010.

Bettadpur, S.: CSR Level-2 Processing Standards Document for Product Release 04, GRACE 327-742, Revision 3.1, The GRACE Project, Center for Space Research, University of Texas at Austin, 2007.

Clark, P. U., Clague, J. J., Curry, B. B., Dreimanis, A., Hicock, S. R., Miller, G. H., Berger, G. W., Eyles, N., Lamothe, M., Miller, B. B., Mott, R. J., Oldale, R. N., Stea, R. R., Szabo, J. P., Thorleifson, L. H., and Vincent, J. S.: Initiation and development of the Laurentide and Cordilleran Ice Sheets following the last interglaciation, Quat. Sci. Rev., 12, 79–114, 1993.

Long-term contributions of Baffin and Bylot Island Glaciers

A. S. Gardner et al.

Dowdeswell, E. K., Dowdeswell, J. A., and Cawkwell, F.: On the glaciers of Bylot Island, Nunavut, Arctic Canada, Arc. Antarct. Alp. Res., 39, 402–411, 2007.

Fisher, D., Zheng, J., Burgess, D., Zdanowicz, C., Kinnard, C., Sharp, M., and Bourgeois, J.: Recent melt rates of Canadian Arctic ice caps are the highest in four millennia, Global Planet. Change, 84–85, 2012.

Fisher, D. A., Koerner, R. M., Bourgeois, J. C., Zielinski, G., Wake, C., Hammer, C. U., Clausen, H. B., Gundestrup, N., Johnsen, S., Goto-Azuma, K., Hondoh, T., Blake, E., and Gerasimoff, M.: Penny ice cap cores, Baffin Island, Canada, and the Wisconsinan Foxe Dome connection: Two states of Hudson Bay ice cover, Science, 279, 692–695, 1998.

Flanner, M. G. and Zender, C. S.: Linking snowpack microphysics and albedo evolution, J. Geophys. Res.-Atmos., 111, doi:10.1029/2005JD006834, 2006.

Fricker, H. A., Borsa, A., Minster, B., Carabajal, C., Quinn, K., and Bills, B.: Assessment of ICESat performance at the Salar de Uyuni, Bolivia, Geophys. Res. Lett., 32, 10.1029/2005gl023423, 2005.

Gardner, A. S. and Sharp, M. J.: Sensitivity of net mass balance estimates to near-surface temperature lapse rates when employing the degree-day method to estimate glacier melt, Ann. Glaciol., 50, 80–86, 2009.

Gardner, A. S. and Sharp, M. J.: A review of snow and ice albedo and the development of a new physically based broadband albedo parameterization, J. Geophys. Res., 115, F01009, doi:10.1029/2009jf001444, 2010.

Gardner, A. S., Moholdt, G., Wouters, B., Wolken, G. J., Burgess, D. O., Sharp, M. J., Cogley, J. G., Braun, C., and Labine, C.: Sharply increased mass loss from glaciers and ice caps in the Canadian Arctic Archipelago, Nature, 473, 357–360, doi:10.1038/nature10089, 2011.

Holdsworth, G.: Evidence of a Surge on Barnes Ice Cap, Baffin Island, Can. J. Earth Sci., 10, 1565–1574, doi:10.1139/e73-148, 1973.

Holdsworth, G.: Surge activity on the Barnes Ice Cap, Nature, 269, 588–590, 1977.

Holdsworth, G.: Glaciological reconnaissance of an ice core drilling site, Penny Ice Cap, Baffin Island, J. Glaciol., 30, 3–15, 1984.

Hooke, R. and Le, B.: Pleistocene ice at the base of the Barnes Ice Cap, Baffin Island, NWT, Canada, J. Glaciol., 17, 49–59, 1976.

Hooke, R. L., Johnson, G. W., Brugger, K. A., Hanson, B., and Holdsworth, G.: Changes in mass balance, velocity, and surface profile along a flow line on Barnes Ice Cap, 1970–1984, Can. J. Earth Sci., 24, 1550–1561, 1987.

Long-term contributions of Baffin and Bylot Island Glaciers

A. S. Gardner et al.

Ivins, E. R., Watkins, M. M., Yuan, D.-N., Dietrich, R., Casassa, G., and Rülke, A.: On-land ice loss and glacial isostatic adjustment at the Drake Passage: 2003–2009, J. Geophys. Res., 116, B02403, doi:10.1029/2010jb007607, 2011.

Jacob, T., Wahr, J., Pfeffer, W. T., and Swenson, S.: Recent contributions of glaciers and ice caps to sea level rise, Nature, 482, 514–518, doi:10.1038/nature10847, 2012.

Jacobs, J. D., Heron, R., and Luther, J. E.: Recent changes at the northwest margin of the Barnes Ice Cap, Baffin Island, N.WT, Canada, Arctic Alpine Res., 25, 341-352, 10.2307/1551917, 1993.

Jacobs, J. D., Simms, E. L., and Simms, A.: Recession of the southern part of Barnes Ice Cap, Baffin Island, Canada, between 1961 and 1993, determined from digital mapping of Landsat TM, J. Glaciol., 43, 98–102, 1997.

Kalnay, E., Kanamitsu, M., Kistler, R., Collins, W., Deaven, D., Gandin, L., Iredell, M., Saha, S., White, G., Woollen, J., Zhu, Y., Chelliah, M., Ebisuzaki, W., Higgins, W., Janowiak, J., Mo, K. C., Ropelewski, C., Wang, J., Leetmaa, A., Reynolds, R., Jenne, R., and Joseph, D.: The NCEP/NCAR 40-year reanalysis project, B. Am. Meteorol. Soc., 77, 437–471, 1996.

Korona, J., Berthier, E., Bernard, M., RÈmy, F., and Thouvenot, E.: SPIRIT. SPOT 5 stereoscopic survey of Polar Ice: Reference Images and Topographies during the fourth International Polar Year (2007–2009), ISPRS J. Photogr. Remote Sens., 64, 204–212, 2009.

Krabill, W., Abdalati, W., Frederick, E., Manizade, S., Martin, C., Sonntag, J., Swift, R., Thomas, R., Wright, W., and Yungel, J.: Greenland Ice Sheet: High-elevation balance and peripheral thinning, Science, 289, 428–430, doi:10.1126/science.289.5478.428, 2000.

Krabill, W. B., Abdalati, W., Frederick, E. B., Manizade, S. S., Martin, C. F., Sonntag, J. G., Swift, R. N., Thomas, R. H., and Yungel, J. G.: Aircraft laser altimetry measurement of elevation changes of the Greenland Ice Sheet: Technique and accuracy assessment, J. Geodyn., 34, 357–376, doi:10.1016/s0264-3707(02)00040-6, 2002.

Krabill, W. B.: IceBridge ATM L2 Icessn Elevation, Slope, and Roughness, (May 1995; May to June 2000; May 2005; May 2011). Boulder, Colorado USA: National Snow and Ice Data Center, Digital media, 2011.

Lambeck, K., Antonioli, F., Purcell, A., and Silenzi, S.: Sea-level change along the Italian coast for the past 10,000 yr, Quat. Sci. Rev., 23, 1567–1598, doi:10.1016/j.quascirev.2004.02.009, 2004.

Løken, O. and Sagar, R.: Mass balance observations on the Barnes Ice Cap, Baffin Island, Canada, Int. Assoc. Sci. Hydrol. Publ., 79, 282–291, 1967.

Long-term contributions of Baffin and Bylot Island Glaciers

A. S. Gardner et al.

Title Page

Abstract	Introduction
Conclusions	References
Tables	Figures

◀◀   ▶▶

◀   ▶

Back   Close

Full Screen / Esc

Printer-friendly Version

Interactive Discussion

Mekis, E. and Hogg, W. D.: Rehabilitation and analysis of Canadian daily precipitation time series, Atmos. Ocean, 37, 53–85, 1999.

Mekis, E. and Vincent, L. A.: An overview of the second generation adjusted daily precipitation dataset for trend analysis in Canada, Atmos. Ocean, 49, 163–177, doi:10.1080/07055900.2011.583910, 2011.

Moholdt, G., Nuth, C., Hagen, J. O., and Kohler, J.: Recent elevation changes of Svalbard glaciers derived from ICESat laser altimetry, Remote Sens. Environ., 114, 2756–2767, 2010.

Nuth, C., Moholdt, G., Kohler, J., Hagen, J. O., and Kääb, A.: Svalbard glacier elevation changes and contribution to sea level rise, J. Geophys. Res., 115, F01008, doi:10.1029/2008jf001223, 2010.

Nuth, C. and K"a"ab, A.: Co-registration and bias corrections of satellite elevation data sets for quantifying glacier thickness change, The Cryosphere, 5, 271–290, doi:10.5194/tc-5-271-2011, 2011.

Ommanney, C. S. L.: The Canadian glacier inventory, In Glaciers, Proceedings of Workshop Seminar 1970, Vancouver, B.C. Ottawa, Ont., 24–25 September 1970, 1971.

Orvig, S.: The Climate of the ablation period on the Barnes Ice-Cap in 1950, Geogr. Ann. A, 33, 166–209, 1951.

Orvig, S.: Glacial-meteorological observations on Icecaps in Baffin Island, Geogr. Ann. A, 36, 193–318, 1954.

Paul, F. and Svoboda, F.: A new glacier inventory on southern Baffin Island, Canada, from ASTER data: II. Data analysis, glacier change and applications, Ann. Glaciol., 50, 22–31, 2009.

Peltier, W. R.: Global glacial isostasy and the surface of the ice-age Earth: The ICE-5G (VM2) model and GRACE, Annu. Rev. Earth Planet. Sci., 32, 111–149, doi:10.1146/Annurev.Earth.32.082503.144359, 2004.

Riva, R. E. M., Gunter, B. C., Urban, T. J., Vermeersen, B. L. A., Lindenbergh, R. C., Helsen, M. M., Bamber, J. L., de Wal, R. S. W. V., van den Broeke, M. R., and Schutz, B. E.: Glacial isostatic adjustment over Antarctica from combined ICESat and GRACE satellite data, Earth Planet. Sci. Lett., 288, 516–523, doi:10.1016/J.Epsl.2009.10.013, 2009.

Rodell, M., Houser, P. R., Jambor, U., Gottschalck, J., Mitchell, K., Meng, C. J., Arsenault, K., Cosgrove, B., Radakovich, J., Bosilovich, M., Entin, J. K., Walker, J. P., Lohmann, D., and Toll, D.: The Global Land Data Assimilation System, B. Am. Meteorol. Soc., 85, 381–394, doi:10.1175/bams-85-3-381, 2004.

Rolstad, C., Haug, T., and Denby, B.: Spatially integrated geodetic glacier mass balance and its uncertainty based on geostatistical analysis: Application to the Western Svartisen Ice Cap, Norway, J. Glaciol., 55, 666–680, 2009.

Sagar, R.: Glaciological and climatological studies on the Barnes Ice Cap, 1962–64, Geogr. Bull., 8, 3–47, 1966.

Schutz, B. E., Zwally, H. J., Shuman, C. A., Hancock, D., and DiMarzio, J. P.: Overview of the ICESat mission, Geophys. Res. Lett., 32, doi:10.1029/2005gl024009, 2005.

Siegfried, M. R., Hawley, R. L., and Burkhart, J. F.: High-resolution ground-based GPS measurements show intercampaign bias in ICESat elevation data near summit, Greenland, IEEE T Geosci. Remote, 49, 3393–3400, 2011.

Smith, B. E., Fricker, H. A., Joughin, I. R., and Tulaczyk, S.: An inventory of active subglacial lakes in Antarctica detected by ICESat (2003–2008), J. Glaciol., 55, 573–595, 2009.

Sneed, W. A., Hooke, R. L., and Hamilton, G. S.: Thinning of the south dome of Barnes Ice Cap, Arctic Canada, over the past two decades, Geology, 36, 71–74, 2008.

Swenson, S. and Wahr, J.: Methods for inferring regional surface-mass anomalies from Gravity Recovery and Climate Experiment (GRACE) measurements of time-variable gravity, J. Geophys. Res., 107, 2193, doi:10.1029/2001jb000576, 2002.

Tushingham, A. M. and Peltier, W. R.: IIce-3G: A new global model of late Pleistocene deglaciation based upon geophysical predictions of post-glacial relative sea level change, J. Geophys. Res., 96, 4497–4523, 1991.

Vincent, L. A., Zhang, X., Bonsal, B. R., and Hogg, W. D.: Homogenization of daily temperatures over Canada, J. Climate, 15, 1322–1334, doi:10.1175/1520-0442(2002)015<1322:hodtoc>2.0.co;2, 2002.

Wahr, J., Molenaar, M., and Bryan, F.: Time variability of the Earth's gravity field: Hydrological and oceanic effects and their possible detection using GRACE, J. Geophys. Res., 103, 30205–30229, doi:10.1029/98JB02844 1998.

Ward, W.: Glaciological studies in the Penny Highland, Baffin Island, 1953, IAHS, General Assembly of Rome, 4, 297–308, 1954.

Weaver, R. L.: "Boas" Glacier (Baffin Island, N.W.T., Canada) mass balance for the five budget years 1969 to 1974, Arctic Alpine Res., 7, 279–284, 1975.

Wouters, B. and Schrama, E. J. O.: Improved accuracy of GRACE gravity solutions through empirical orthogonal function filtering of spherical harmonics, Geophys. Res. Lett., 34, L23711, doi:10.1029/2007gl032098, 2007.

Long-term contributions of Baffin and Bylot Island Glaciers

A. S. Gardner et al.

Title Page

Abstract | Introduction

Conclusions | References

Tables | Figures

◄ | ►

Back | Close

Full Screen / Esc

Printer-friendly Version

Interactive Discussion

Wouters, B., Chambers, D., and Schrama, E. J. O.: GRACE observes small-scale mass loss in Greenland, Geophys. Res. Lett., 35, L20501, doi:10.1029/2008GL034816, 2008.

Zdanowicz, C., Smetny-Sowa, A., Fisher, D., Schaffer, N., Copland, L., Eley, J., and Dupont, F.: Summer melt rates on Penny Ice Cap, Baffin Island: Past and recent trends and implications for regional climate, J. Geophys. Res., 117(F2), F02006, doi:10.1029/2011JF002248, 2012.

Zdanowicz, C. M., Fisher, D. A., Clark, I., and Lacelle, D.: An ice-marginal delta O-18 record from Barnes Ice Cap, Baffin Island, Canada, Ann. Glaciol., 35, 145–149, doi:10.3189/172756402781817031, 2002.

Zwally, H. J., Schutz, B., Abdalati, W., Abshire, J., Bentley, C., Brenner, A., Bufton, J., Dezio, J., Hancock, D., Harding, D., Herring, T., Minster, B., Quinn, K., Palm, S., Spinhirne, J., and Thomas, R.: ICESat's laser measurements of polar ice, atmosphere, ocean, and land, J. Geodyn., 34, 405–445, 2002.

Zwally, H. J., Jun, L., Brenner, A. C., Beckley, M., Cornejo, H. G., DiMarzio, J., Giovinetto, M. B., Neumann, T. A., Robbins, J., and Saba, J. L.: Greenland ice sheet mass balance: Distribution of increased mass loss with climate warming; 2003–07 versus 1992–2002, J. Glaciol., 57, 88–102, 2011a.

Zwally, H. J., Schutz, R., Bentley, C., Bufton, J., Herring, T., Minster, B., Spinhirne, J., and Thomas, R.: GLAS/ICESat L1B Global Elevation Data V031, 20 February 2003 to 11 October 2009, National Snow and Ice Data Center, Boulder, CO, Digital media, 2011b.

Title Page

Abstract | Introduction

Conclusions | References

Tables | Figures

◀ | ▶

◀ | ▶

Back | Close

Full Screen / Esc

Printer-friendly Version

Interactive Discussion

Table 1. Glacier mass change determined from CDED, SPOT, ICESat and ATM elevation data sets with respective uncertainties.

method	region	area [km^2]	start date	end date	dM/dt [Gt a^{-1}]	1σ uncertainty [Gt a^{-1}]						
						measurement	GIA	glacier area [±5 %]	extrapolation	bulk density [±25 kg m^{-3}]	20 m density > 1400 m a.s.l	total
SPOT-CDED	Barnes	5863	1960	2010	−2.9	0.26	0.00	0.14	0.00	0.07	0.00	0.31
	Bylot	4875	1979	2008	−1.4	0.39	0.00	0.07	0.07	0.03	0.02	0.40
	Penny	6508	1958	2010	−1.2	0.58	0.00	0.06	0.06	0.03	0.15	0.60
	South	7588	1958	2010	−1.8	0.30	0.00	0.09	0.09	0.05	0.02	0.33
ICESat-CDED	Barnes	5863	1960	2006	−2.5	0.27	0.00	0.13	0.13	0.06	0.00	0.33
	Bylot	4875	1980	2006	−1.3	0.40	0.00	0.06	0.06	0.03	0.02	0.41
	Penny	6508	1958	2006	−1.6	0.27	0.00	0.08	0.19	0.04	0.15	0.37
	North	16121	1963	2006	−4.1	0.37	0.00	0.21	0.25	0.10	0.03	0.50
	South	7588	1957	2006	−1.5	0.19	0.00	0.08	0.05	0.04	0.02	0.21
	All	40955	1962	2006	−11.1	1.49	0.00	0.55	0.68	0.28	0.21	1.83
ATM-CDED	Barnes	5863	1960	1995	−1.9	0.34	0.00	0.10	0.04	0.05	0.00	0.36
ATM-ATM	Barnes	5863	1995	2000	−3.3	0.07	0.02	0.17	0.07	0.08	0.00	0.21
	Penny	6508	1995	2000	−1.3	0.08	0.02	0.06	0.20	0.03	0.29	0.37
	non ice cap	28584	1995	2000	−10.4	0.37	0.08	0.52	3.21	0.26	0.14	3.28
	All	40955	1995	2000	−14.9	0.52	0.11	0.75	3.48	0.37	0.43	3.64
ATM-ATM	Barnes	5863	2000	2005	−4.1	0.07	0.02	0.21	0.08	0.10	0.00	0.26
	Penny	6508	2000	2005	−2.9	0.08	0.02	0.14	0.46	0.07	0.29	0.57
	non ice cap	28584	2000	2005	−18.3	0.37	0.08	0.91	5.66	0.46	0.14	5.77
	All	40955	2000	2005	−25.3	0.52	0.11	1.26	6.21	0.63	0.43	6.40
ATM-ATM	Barnes	5863	2005	2011	−6.2	0.06	0.02	0.31	0.12	0.16	0.00	0.37
ICESat-ICESat	Barnes	5863	2003	2009	−5.0	0.12	0.02	0.25	0.25	0.12	0.00	0.39
	Bylot	4875	2003	2009	−2.7	0.12	0.01	0.14	0.14	0.07	0.04	0.24
	Penny	6464	2003	2009	−3.3	0.14	0.02	0.17	0.17	0.08	0.29	0.41
	North	16109	2003	2009	−8.4	0.27	0.04	0.42	0.42	0.21	0.06	0.69
	South	7588	2003	2009	−5.8	0.16	0.02	0.29	0.29	0.14	0.04	0.46
	All	40899	2003	2009	−25.1	0.81	0.11	1.26	1.26	0.63	0.43	2.10

Table A1. ICESat validation and filtering of SPOT DEMs over glacier free ground (grd) and over glacier ice (ice)

	acquisition date	standard deviation [m]		mean elevation difference [m] (SPOT − ICESat)		ICESat postings over valid cells		elevation dependent	min. acceptable correlation		% cells excluded	
		grd	ice	grd	ice	grd	ice		grd	ice	grd	ice
Barnes_A V1	2008	2.4	3.2	−12.5	−13.2	6593	1721	no	0	0	54	45
Barnes_A V2	2008	2.4	3.8	−12.5	−13.4	6514	974	no	0	0	56	65
Barnes_B V1	2010*	4.9	1.4	1.3	0	1745	499	yes*	75	0	77	17
Barnes_B V2	2010*	4.8	1.4	1.2	0	2569	499	yes*	20	0	66	18
Bylot V1	2008	3.4	5.3	−12.4	−11.3	1087	966	no	85	45	74	24
Bylot V2	2008	3.4	4.6	−12.3	−11.5	1185	914	no	80	5	73	30
Penny V1	2010*	4.2	10.6	−3.8	−4.6	913	119	yes*	40	65	73	54
Penny V2	2010*	5.2	14.2	-3.9	-5.2	952	115	yes*	0	45	73	53
C.P. V1	2010*	2.8	8.6	3	2.4	1911	503	yes*	0	0	61	38
C.P. V2	2010*	2.9	6.6	3	1.5	1877	388	yes*	0	30	63	49
Baffin N V1	2010*	4	1.1	4.8	5	2427	187	yes*	65	80	72	38
Baffin N V2	2010*	4.5	2.9	4.9	5.3	2647	210	yes*	5	0	70	30

* 2010 SPOT DEMs were compared with 2009 ICESat altimetry (last year of operation). Observed elevationally dependent bias is consistent with expected changes in glacier elevations between acquisition dates so no correction is applied.

A. S. Gardner et al.

Table A2. Comparison of CDED with ICESat and SPOT elevations over ground before and after co-registration and elevation bias corrections.

	acquisition date	standard deviation [m]		mean difference [m] (ICESat/SPOT – CDED)		acceptable grid cells/postings	horizontal misalignment [m]
		before	after	before	after		
ICESat	2004–2008	5.1	4.8	−1.1	0.0	176 248	0
Barnes_A V1	2008	5.4	4.9	−14.7	0.0	3 310 359	19
Barnes_A V2	2008	5.3	4.8	−14.7	0.0	3 228 148	18
Barnes_B V1	2010	5.8	5.5	−1.3	0.1	1 807 496	17
Barnes_B V2	2010	5.8	5.5	−1.5	0.0	2 698 810	17
Bylot V1	2008	7.0	5.5	−11.6	0.2	1 116 149	29
Bylot V2	2008	6.7	5.2	−11.7	0.2	1 195 762	29
Penny V1	2010	13.7	13.0	−6.3	−0.8	2 077 339	8
Penny V2	2010	11.8	11.1	−6.2	−0.7	2 033 699	7
C.P. V1	2010	8.9	8.2	−0.3	−0.6	3 151 766	11
C.P. V2	2010	8.0	7.4	−0.4	−0.6	2 992 215	11
Baffin N V1	2010	10.2	9.0	1.8	−0.8	1 589 012	16
Baffin N V2	2010	9.7	8.5	2.0	−0.6	1 757 755	16
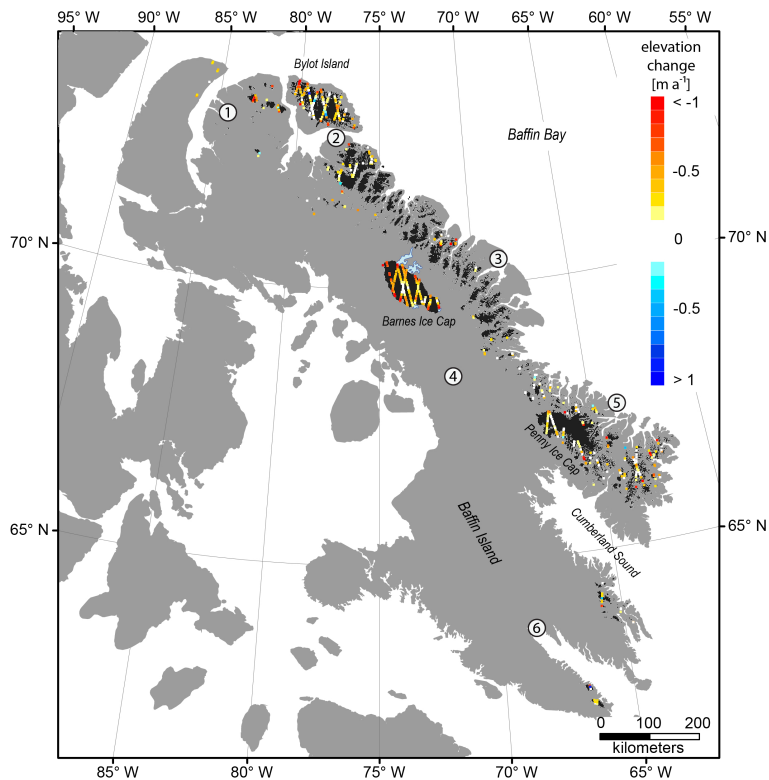
Fig. 1. Elevation change (m a^{-1}) between 1965 and 2006 as determined from ICESat satellite laser altimetry and DEMs generated from airborne stereoscopic imagery (CDED). Numbered dots show the locations of the Environment Canada weather stations used to characterize regional climate [Nanisivik (1), Pond Inlet (2), Clyde River (3), Dewar Lakes (4), Fox Five (5) and Iqaluit (6)].

Title Page

Abstract | Introduction

Conclusions | References

Tables | Figures

⏮ | ⏭

◀ | ▶

Back | Close

Full Screen / Esc

Printer-friendly Version

Interactive Discussion
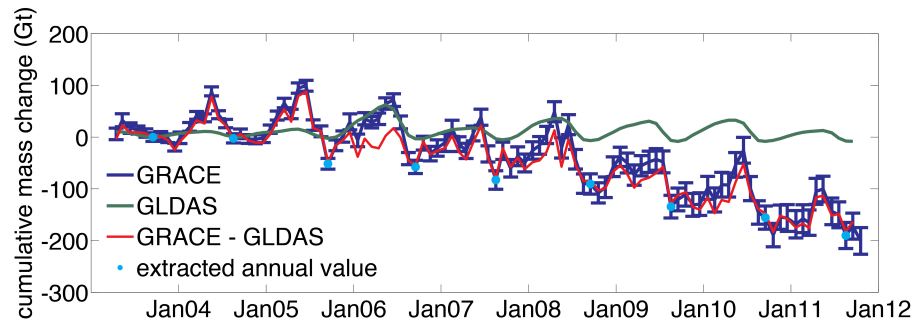
Fig. 2. Baffin and Bylot Island monthly cumulative mass change from GRACE shown in blue (±1σ), from GLDAS shown in green, and for GRACE corrected with GLDAS shown in red. Cyan dots show summer minima selected as annual markers.
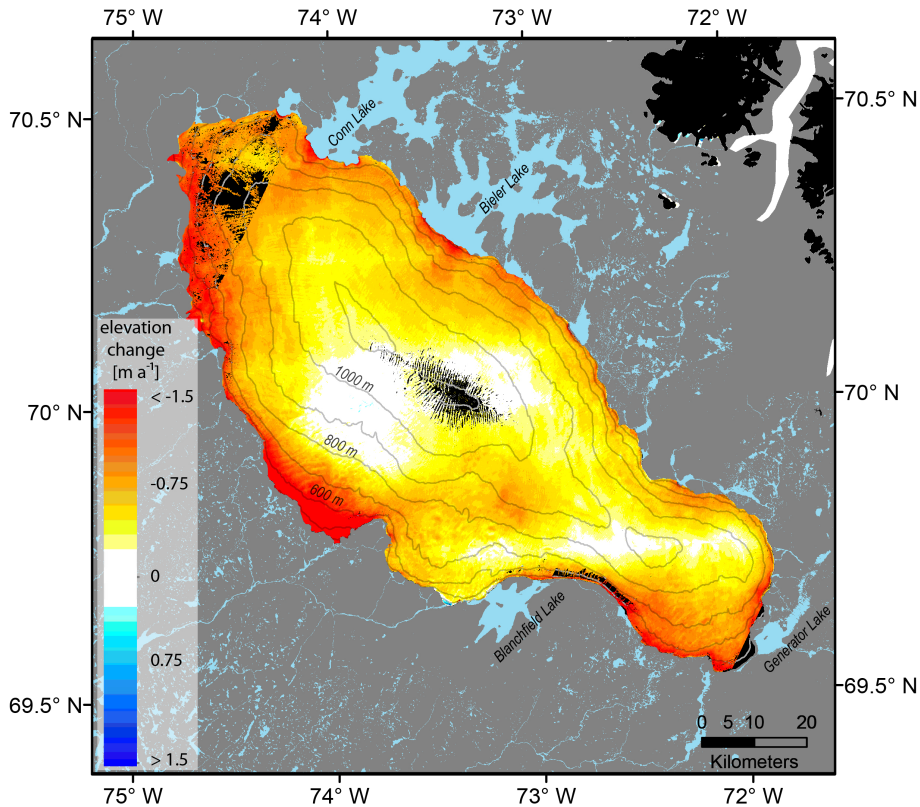
Fig. 3. Elevation change (m a^{-1}) of the Barnes Ice Cap between 1960 and 2010 as determined from DEMs generated from airborne and SPOT-5 satellite stereoscopic imagery. Areas of black indicate no data.

Long-term contributions of Baffin and Bylot Island Glaciers

A. S. Gardner et al.

Title Page

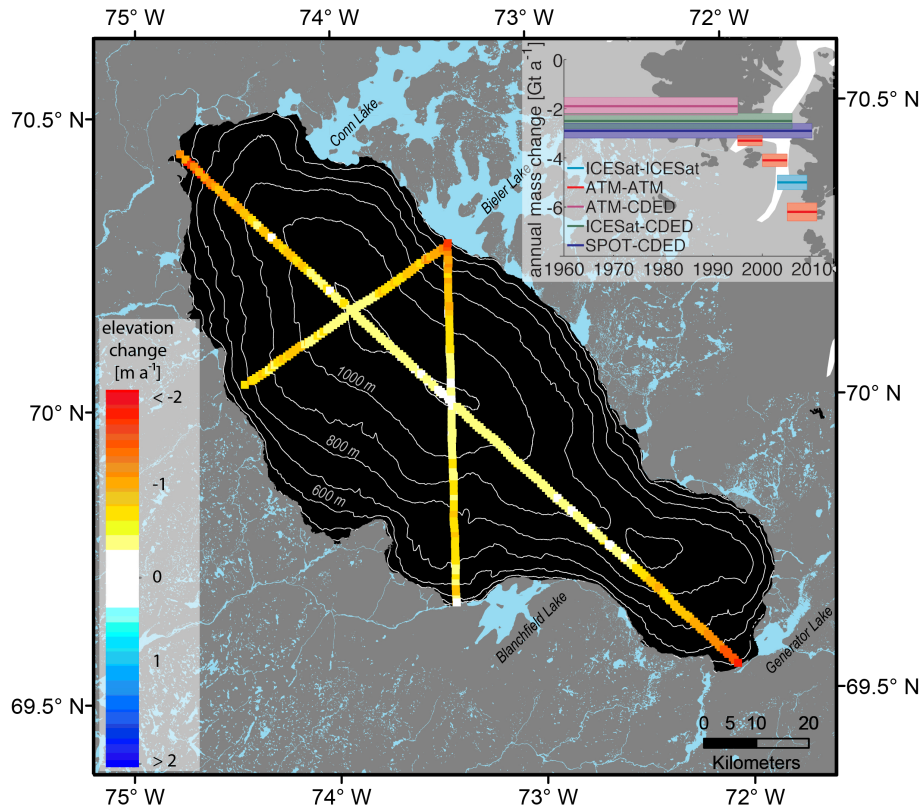| Abstract | Introduction |
| Conclusions | References |
| Tables | Figures |

Back | Close

Full Screen / Esc

Printer-friendly Version

Interactive Discussion
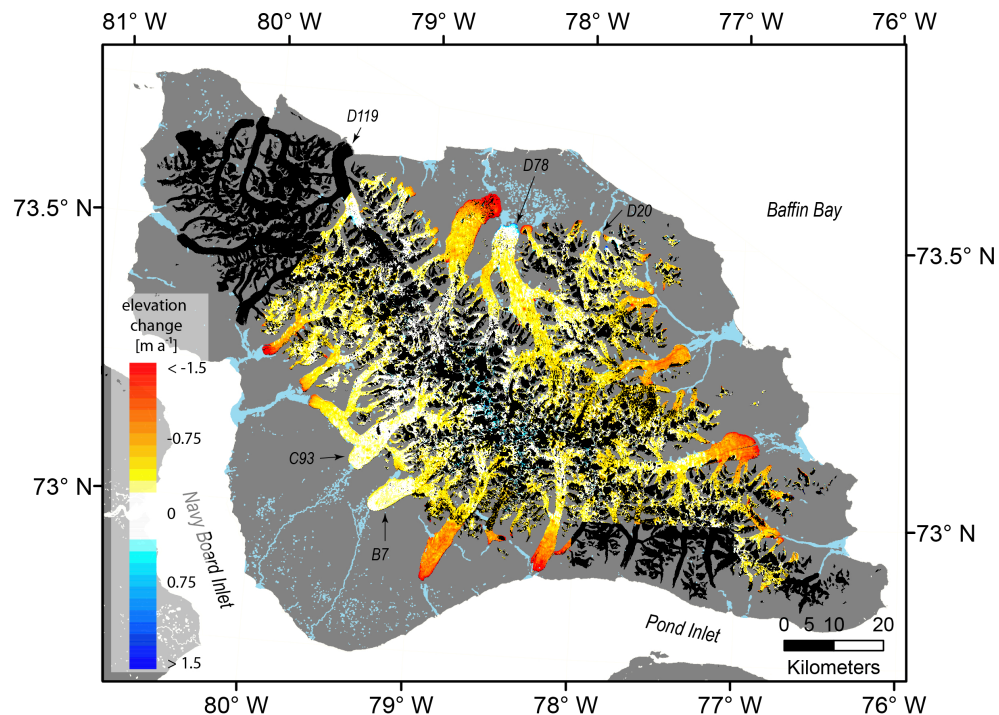
Fig. 4. Elevation change rate (m a^{-1}) of the glaciers of Bylot Island between 1979 and 2008 as determined from DEMs generated from airborne and SPOT-5 satellite stereoscopic imagery. Areas of black indicate no data.

Long-term contributions of Baffin and Bylot Island Glaciers

A. S. Gardner et al.

Title Page

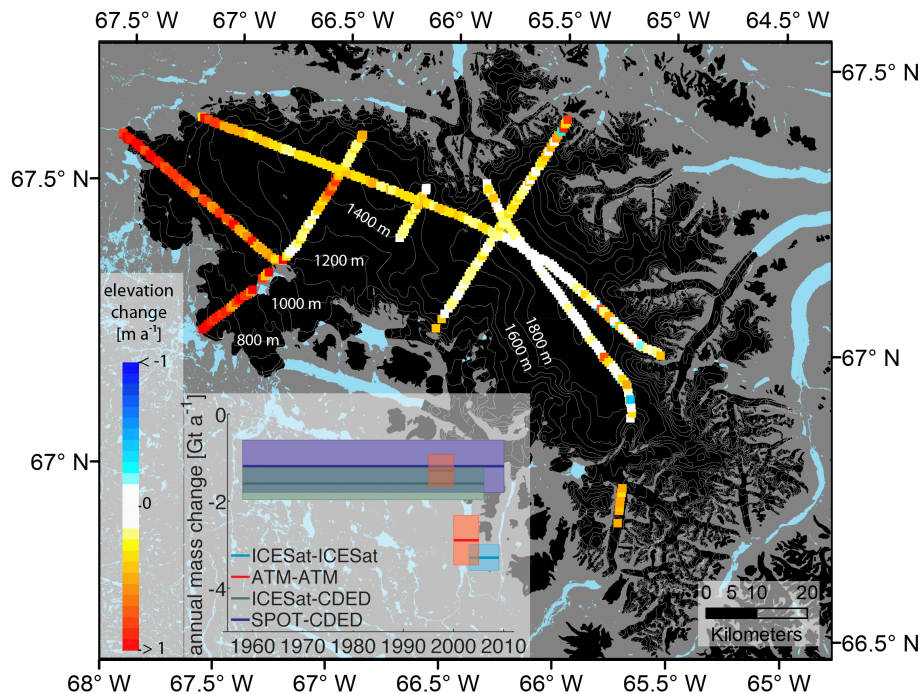| Abstract | Introduction |
| Conclusions | References |
| Tables | Figures |

|◄ | ►|

◄ | ►

Back | Close

Full Screen / Esc

Printer-friendly Version

Interactive Discussion
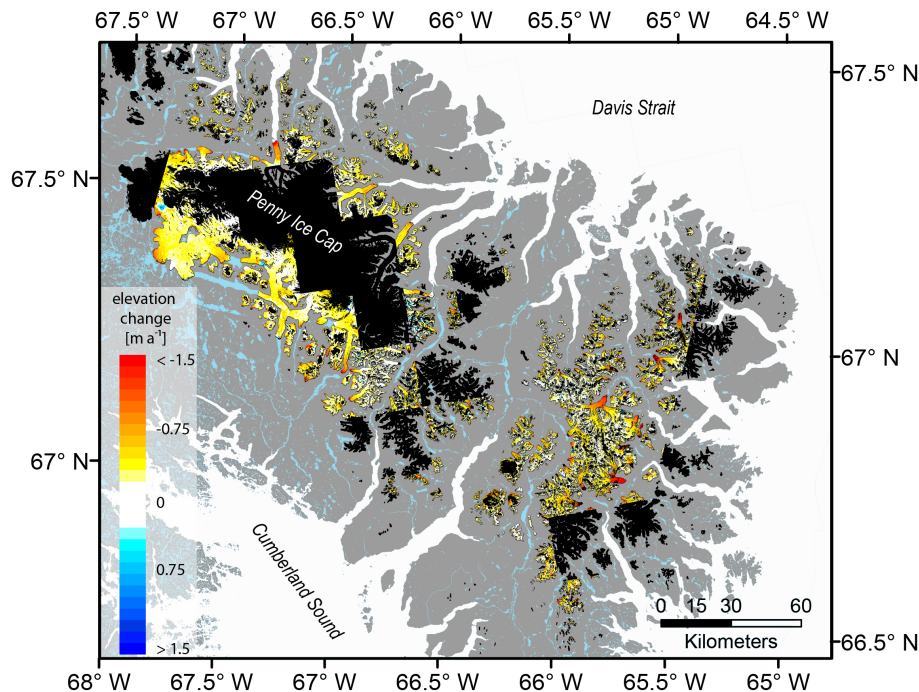
Fig. 5. Elevation change rate $(\mathrm{m\,a^{-1}})$ of the Penny Ice Cap and the glaciers of the Cumberland Peninsula between 1958 and 2010 as determined from DEMs generated from airborne and SPOT-5 satellite stereoscopic imagery. Areas of black indicate no data.

Fig. 6. Elevation change rate ($\mathrm{m\,a^{-1}}$) of the Barnes Ice Cap between Spring 2000 and Spring 2005 as determined from repeat airborne laser altimetry. Inset graph shows annual mass change of the Barnes Ice Cap determined over varying time intervals.

Title Page

Abstract | Introduction

Conclusions | References

Tables | Figures

|◀ | ▶|

◀ | ▶

Back | Close

Full Screen / Esc

Printer-friendly Version

Interactive Discussion

Fig. 7. Elevation change rate (m a^{-1}) of the Penny Ice Cap between Spring 2000 and Spring 2005 as determined from repeat airborne laser altimetry. Inset graph shows annual mass change of the Penny Ice Cap determined over varying time intervals.

Title Page

Abstract | Introduction

Conclusions | References

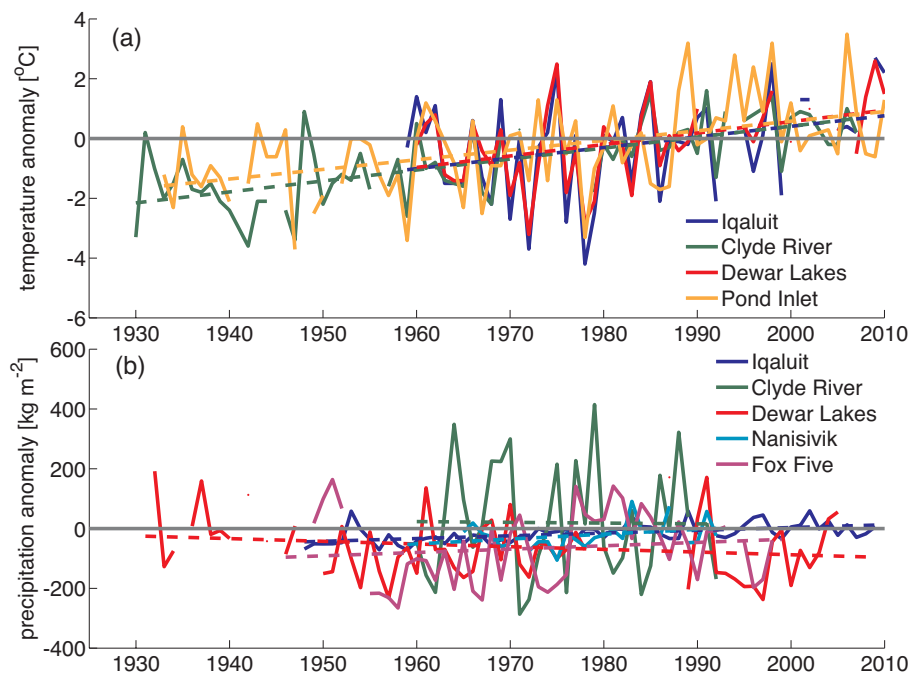Tables | Figures

◄◄ | ►►

◄ | ►

Back | Close

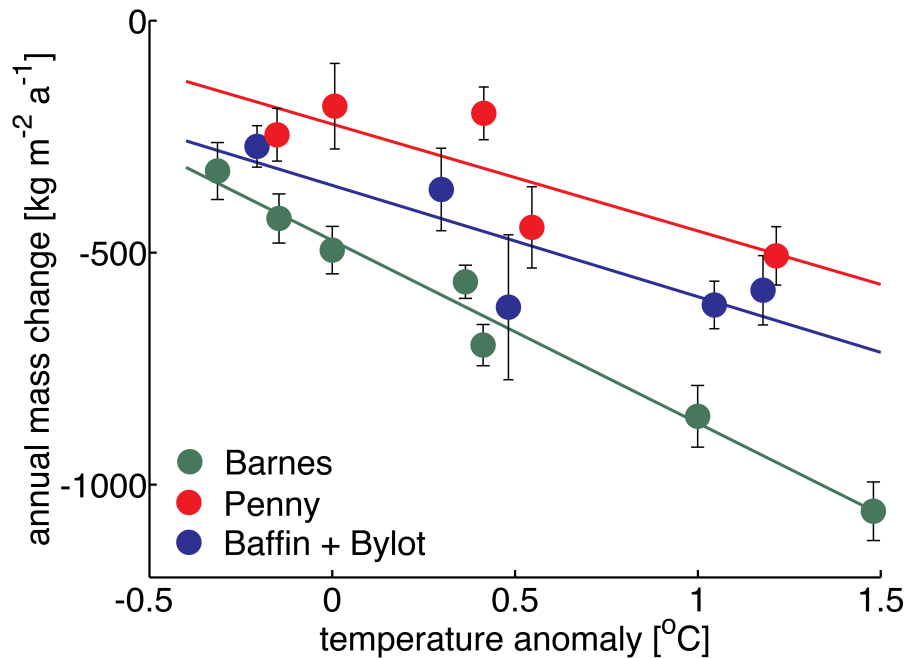Full Screen / Esc

Printer-friendly Version

Interactive Discussion

Fig. 8. (a) Temperature and **(b)** precipitation anomalies relative to the 1981–1990 mean (optimal period of overlap). Dashed lines show linear trends fitted to all data from each station.

Fig. 9. Annual mass change ($\pm 1\sigma$) plotted against NCEP R1 summer (J,J,A) glacier area-averaged 700 mb temperature anomalies averaged over each mass change measurement interval. Anomalies are relative to the 1960–2010 means. Lines show linear fits with slopes of: Barnes = −390 ($r = -0.99$), Penny = −230 ($r = -0.83$), and Baffin and Bylot Island glaciers = −240 ($r = -0.84$) with units of $\mathrm{kg\,m^{-2}\,a^{-1}}$ per 1 °C increase in temperature.

Fig. 10. Mass changes of Baffin and Bylot Island Glaciers (±1σ).

Discussion Paper | Discussion Paper | Discussion Paper | Discussion Paper

TCD

6, 1563–1610, 2012

Long-term contributions of Baffin and Bylot Island Glaciers

A. S. Gardner et al.

Title Page

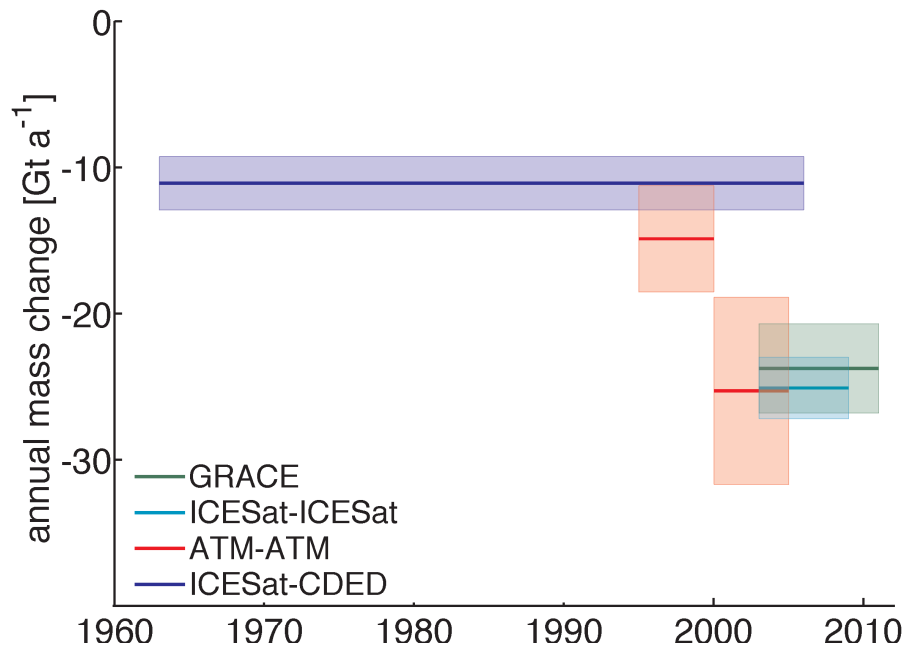| Abstract | Introduction |
| Conclusions | References |
| Tables | Figures |

|◄ | ►|

◄ | ►

Back | Close

Full Screen / Esc

Printer-friendly Version

Interactive Discussion

Fig. A1. Workflow for SPOT DEM validation and filtering using ICESat altimetry.

Fig. A2. Workflow for SPOT-CDED differencing.

The flowchart contains the following boxes:

- Single SPOT-5 40 m DEM [adjusted according to SPOT – ICESat workflow]
- reference to WGS84 ellipsoid (EGM96 Geopotential Model)
- exclude interpolated pixels
- All 1:50k CDEDs within spatial limits of SPOT DEM
- mosaic CDEDs
- project and resample to SPOT DEM grid
- reference to WGS84 ellipsoid (HT2.0 geoid model)
- filter points, exclude: enddate > 1983
- dh = SPOT - DEM
- identify grid cells over ice (dh_{ice}), all points outside of 1km buffer surrounding ice = ground (dh_{grd})
- filter dH by SPOT correlation score (CS), exclude: $CS_{ice} < CS_{min\_ice}$ & $CS_{grd} < Cs_{min\_grd}$
- filter out outliers: $dh_{grd} > 3 \times std(dh_{grd})$ & $dh_{ice} > 3 \times std(dh_{ice})$
- check for horizontal misalignment and vertical offset over ground using the trigonometric relationship between slope, aspect, and dh_{grd} (determined from medians of 5° aspect bins for slopes > 2°)
- if improvement in the standard deviation of dh_{grd} > 1% and the magnitude of the shift is > 1 meter
- shift SPOT DEM
- TRUE
- FALSE
- correct for slope dependent bias using a third-order polynomial fit to slope vs. dh_{grd}
- Correct for spatially dependent elevation bias. Median dh_{grd} for all grid cells of a 100 km by 100 km grid are determined. Cells with < 500 grid cells are linearly interpolated from neighboring cells. Cells that can not be interpolated are set using a plane fit to all filled grid values. The coarse gird is then interpolated to SPOT DEM grid using cubic spline interpolation.
- FINISH

Fig. A3. Workflow for ICESat-CDED differencing.

Title Page

Abstract | Introduction

Conclusions | References

Tables | Figures

◄ | ►

Back | Close

Full Screen / Esc
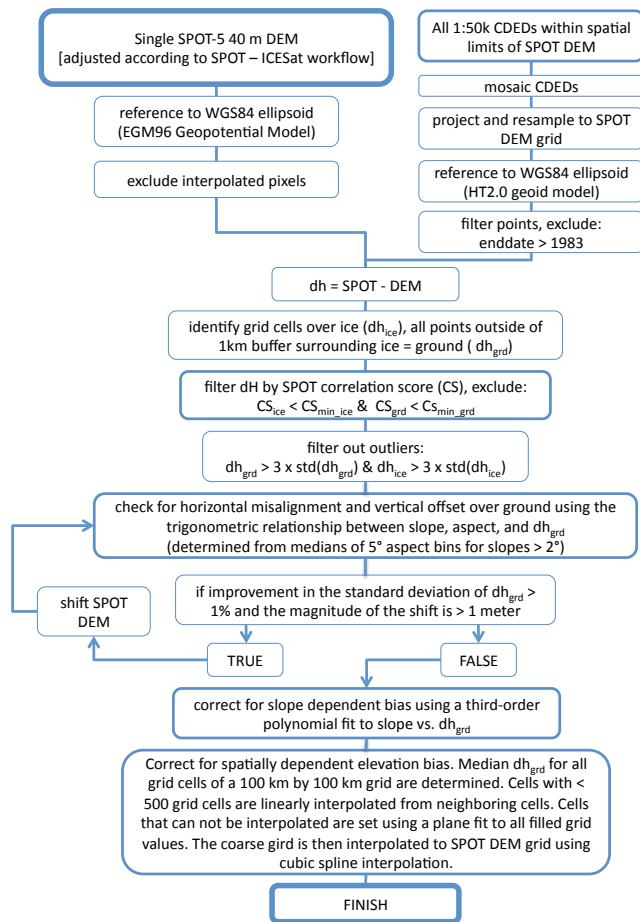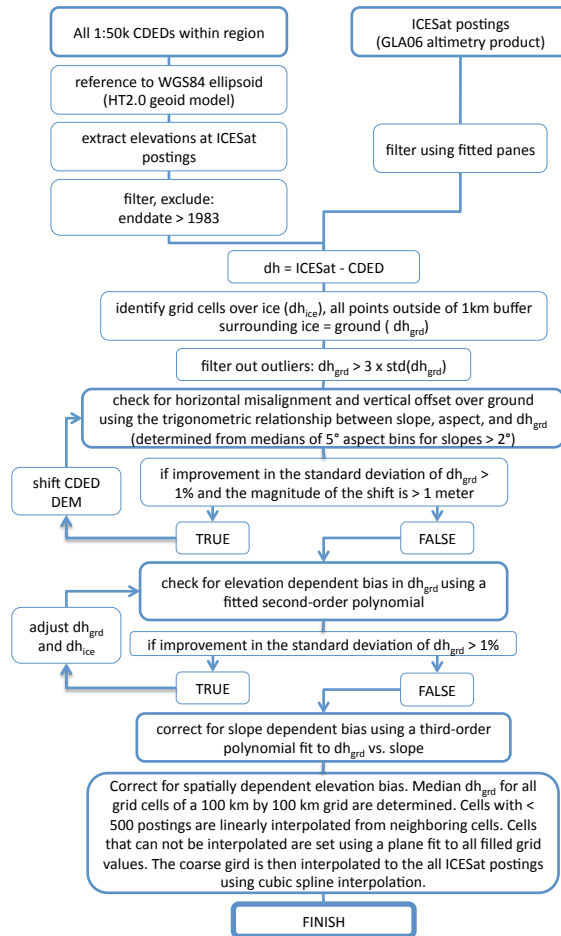
Printer-friendly Version

Interactive Discussion